Coupling models of within-human, human-to-mosquito, and within-mosquito malaria parasite dynamics to identify key drivers of malaria transmission

Xiao Sun[1], Matthew WA Dixon[2,3], James S McCarthy[2,3,4], James M McCaw *[1,5], and Pengxing Cao †[1]

[1]School of Mathematics and Statistics, The University of Melbourne, Melbourne, VIC, Australia
[2]Department of Infectious Diseases, The Peter Doherty Institute, The University of Melbourne, Parkville, VIC, Australia
[3]Walter and Eliza Hall Institute, Parkville, VIC, Australia
[4]Victorian Infectious Diseases Service, The Royal Melbourne Hospital, Parkville, Victoria, Australia
[5]Melbourne School of Population and Global Health, The University of Melbourne, Melbourne, VIC, Australia

Abstract

Malaria is a public health burden affecting billions of people worldwide. Transmission of malaria parasites from the human host to the mosquito during a blood meal is an essential step in the life cycle of the parasite. Quantitative estimation of the contributions of different host factors to human-to-mosquito transmission is essential for a mechanistic understanding of the biological processes underpinning malaria transmission. In this study, we develop a multi-scale stochastic model of human-to-mosquito transmission by coupling a model of within-human parasite dynamics with a model describing malaria transmission and sexual development within the mosquito host. We fit the model to data from a direct feeding assay that formed part of a human challenge study. We use a Bayesian statistical approach to estimate several biological parameters that have until now been difficult to quantify in the literature and conducted a sensitivity analysis to identify the critical factors that influence the probability of human-to-mosquito transmission. Our results show that (1) the number of viable male gametes developing within a mosquito is approximately 80% (95% uncertainty: 13%–290%) of the total number of male gameto-

*jamesm@unimelb.edu.au
†pengxing.cao@unimelb.edu.au

cytes taken in a blood meal and the probability of successful fertilization between a female gamete and a viable male gamete is approximately 2.90% (0.57%–10.92%); and (2) the leading factors influencing the probability of human-to-mosquito transmission are the multiplication factor of asexual parasites and the maturation rate of gametocytes within the human host. We also show that, for asymptomatic infections where asexual parasitemia oscillates around an approximate level after the exponential growth phase, the probability of parasite transmission from an asymptomatic individual to mosquitoes is strongly correlated with the parasitemia level, validating the link between asexual parasitemia and the transmission probability. Our work not only provides a better mechanistic understanding of the biological processes underpinning malaria transmission but also provides a framework that—by combining data and mathematical and statistical approaches—can be integrated into a multi-scale epidemiological transmission model to evaluate and develop more effective intervention strategies in support of efforts to eliminate malaria.

Author summary

Malaria is a life-threatening disease. The human-to-mosquito transmission occurs when a mosquito feeds on the blood of the infected individual and ingests gametocytes. Although a higher concentration of circulating gametocytes in the human blood stream is associated with a higher probability of human-to-mosquito transmission, it is unclear how different host factors influence the probability of malaria parasite transmission from a human host to mosquitoes. To investigate this, we develop a stochastic model of human-to-mosquito transmission dynamics that integrates blood-stage parasite dynamics in humans, the uptake of gametocytes by a mosquito during a blood meal, and parasite development within mosquitoes. We use the model to estimate several biological parameters governing the transmission process, identifying the most influential human host factors affecting the gametocytemia level, as well as the mosquito factors that determine the probability of human-to-mosquito transmission for a given gametocytemia level in the infected human host. By combining multiple sources of data with mathematical and statistical approaches to study human-to-mosquito transmission dynamics, our work provides a quantitative mechanistic understanding of the biological processes underpinning malaria transmission. Furthermore, our work will enable the development of a detailed multi-scale epidemiological transmission framework through which novel intervention strategies for the control of malaria transmission can be evaluated.

1 Introduction

Malaria is a vector-transmitted infection that poses a continuing health threat to billions of people worldwide, causing approximately half a million deaths each year [1]. The transmission of malaria parasites from the human host to the mosquito occurs when a female Anopheles mosquito feeds on the blood of the infected individual and ingest at least one male and one female mature gametocyte [2]. Those gametocytes undergo meiosis in the mosquito midgut before developing into sporozoites which move to the salivary gland of the mosquito, enabling their transmission back to a human to cause a new infection. Investigating this process experimentally is conducted using mosquito feeding assays where mosquitoes are allowed to feed on a blood sample containing gametocytes, either through in direct contact with the skin of an infected host (referred to as a direct feeding assay), or on glass containers containing infected blood (membrane or indirect feeding assay). Mosquitoes are then examined for the presence of oocysts or sporozoites. Such assays are widely used to experimentally evaluate both the infectiousness of infected human hosts to mosquitoes and the efficacy of interventions to block transmission such as drugs or vaccines [3–5]. Mosquito feeding assays provide a direct measurement of the probability that a mosquito will become infectious by developing sporozoites after taking a blood meal from a human with circulating gametocytes. Such data, when analyzed using mechanistic models, can provide new insight into the biological processes underpinning malaria transmission.

For falciparum malaria, it has been shown that the proportion of mosquitoes developing sporozoites in mosquito feeding experiments is positively correlated with the level of gametocytes [6–8]. However, it is unclear what the relative importance is among various factors, including those governing the gametocyte development in human hosts and those driving the development of sporozoites in mosquitoes, in determining the probability of human-to-mosquito transmission. It is difficult and costly to design experimental studies that can disentangle the relative importance of each biological factor governing transmission. Mathematical models, calibrated against data, may support new insights into transmission, effectively filling this gap. Many mathematical models have been developed to help understand the life cycle of malaria parasites in either the human host or mosquito. For example, models have been developed to investigate the population dynamics of asexual parasites, evaluate the effectiveness of antimalarial drugs [9–11], explore gametocyte dynamics in humans [12, 13], examine within-mosquito dynamics [14, 15], and estimate the extrinsic incubation period [16, 17]. To date, a model of human-to-mosquito transmission that integrates both within-human parasite dynamics and within-mosquito parasite dynamics has not been described. Furthermore, published models are predominantly deterministic, and therefore not readily

applicable to modeling the real world situations where the level of gametocytemia is low, and where the human-to-mosquito transmission probability can be highly sensitive to the numbers of male and female gametocytes circulating in the blood stream. While a number of stochastic models of within-human parasite dynamics and within-mosquito parasite dynamics have been developed (by us [18] and others [17]), coupling the human and mosquito systems through a probabilistic model for the uptake of female and male gametocytes by mosquitoes during a blood meal remains a major open challenge.

Successfully addressing this modeling and data integration challenge will provide a quantitative analysis of the contributions of human and mosquito factors to human-to-mosquito transmission. Although existing studies—based on experimental data or mosquito feeding assay data [13, 17]—have provided estimates for most of the parameters governing within-human and within-mosquito parasite dynamics, we have identified two biological parameters that are poorly quantified, yet expected to play a significant role in characterizing a successful transmission of the malaria parasite from human to mosquito. One is the number of viable male gametes available for fertilization in the mosquito after blood feeding (because male gametocytes/gametes are usually present in a smaller quantity compared to female ones in blood samples [19], limiting the maximum number of zygotes that can be developed). While it has been known that a male gametocyte can produce up to eight male gametes [20], some of the male gametes produced become defective during the replication/differentiation process, and thus are unable to fertilize female gametes [21–23]. Attrition leads to the number of viable male gametes being possibly fewer than the number of male gametocytes taken by the mosquito through blood feeding. The other parameter that is poorly quantified is the probability of successful fertilization involving viable female and male gametes, which, to the best of our knowledge, has not been estimated.

In this study, we develop a stochastic model of human-to-mosquito transmission that integrates parasite dynamics in both humans and mosquitoes. We first estimate the two aforementioned biological parameters by applying the model to a set of direct feeding assay data from a volunteer infection study (VIS) where human volunteers were infected with *P. falciparum* and subsequently exposed to feeding mosquitoes [24]. The experiment provides unique *in vivo* data of gametocyte concentration and feeding assay outcomes for individual volunteers, enabling the estimation of biological parameters using our stochastic model and approximate Bayesian computation inference methods [25]. We then use the data-calibrated model to simulate direct mosquito feeding assays and conduct a sensitivity analysis to identify how different host factors influence the probability of human-to-mosquito transmission. Finally, we use the model to predict the transmission probability of asymptomatic infections with cyclic parasitemia

at set-point levels in different transmission settings, and quantify the relationship between the level of asexual parasitemia and the probability of human-to-mosquito transmission.

2 Materials and methods

2.1 The model

We will introduce a stochastic model of the human-to-mosquito transmission process. It includes two submodels: one capturing the within-human life cycle of asexual parasites and the development of gametocytes, and the other capturing the process of transmission from human to mosquito and subsequent within-mosquito parasite development.

2.1.1 Within-human parasite dynamics

We extend a previously developed model of within-human parasite dynamics [13, 18] to capture the stochastic process of gametocyte development. A schematic diagram of the within-human model is shown in Fig 1. The model contains three major parasite populations: asexual parasites $P(a,t)$, sexually committed parasites $P_G(a,t)$ and gametocytes (including immature stages $G_1(t)$–$G_4(t)$ and mature male $G_M(t)$ and female $G_F(t)$ populations), where a represents parasite age and t represents time since the onset of blood stage infection. Asexual parasites can invade red blood cells (RBCs) and initiate an asexual life cycle lasting a_L hours, during which they undergo maturation and replication. The parasitized RBCs (pRBC) may die at any time governed by a rate parameter δ_p. If they reach the end of the asexual life cycle, rupture occurs, releasing merozoites which invade uninfected RBCs and initiate a new replication cycle. During the asexual life cycle, a small fraction of the parasites (at age a_s) differentiate into sexually committed parasites and eventually develop into male and female gametocytes.

As the stochastic model is not amenable to analytical study, we simulate it using the tau-leaping algorithm [26]. In detail, we initially calculate the total number of asexual parasites at the time of inoculation $P(a,0)$, which is given by multiplying the initial density parameter P_{init} (see Table 1) by an assumed blood volume V_H of 4000mL. We then distribute the $P(a,0)$ parasites across the a_L age bins by generating $P(a,0)$ random samples from a truncated normal distribution $N_{[1,a_L]}(\mu,\sigma^2)$ and rounding the samples to the nearest integers. Subsequently, the number of asexual parasites evolves according to the

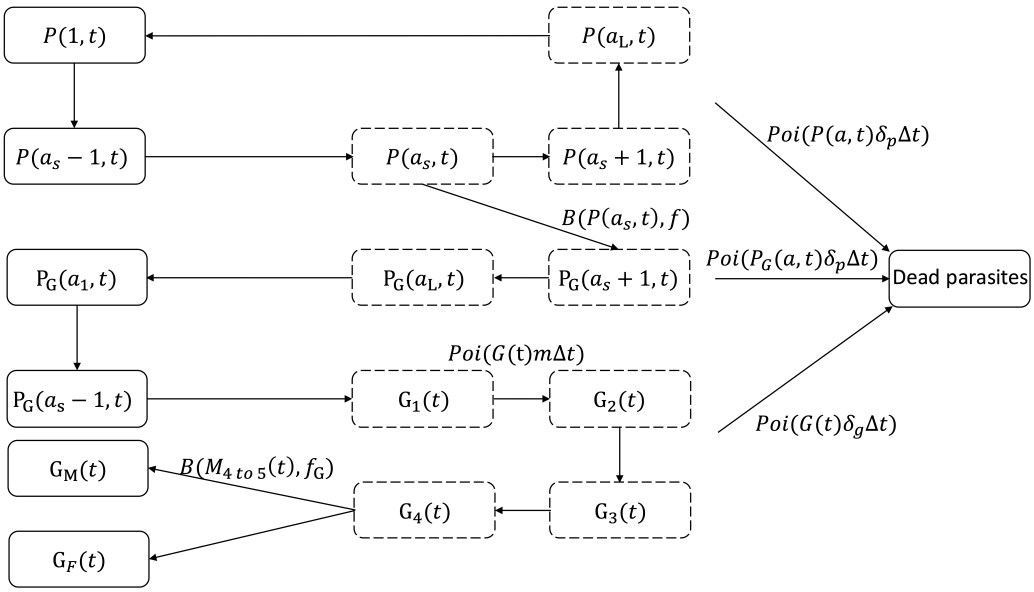

Figure 1: **Within-human model compartments and transitions.** The model contains three major parasite populations: P (asexual parasites), P_G (sexually committed parasites) and G (gametocytes). P and P_G are functions of parasitemia with age a at time t. The loop $P(a,t)$ describes the synchronous waves of asexual replication and maturation in a_L hours. A small fraction f of asexual parasites enter the sexual development cycle when sexual commitment occurs at age a_s, developing into sequestered gametocytes $G_1(t)$–$G_4(t)$ and eventually becoming circulating mature male (G_M) and female (G_F) gametocytes, with probabilities f_G and $1-f_G$ respectively. Parasites may die at any point during the developmental process, following a Poisson process with a probability per unit time (i.e., per time step Δt of one hour) determined by $P(a,t)\delta_p\Delta t$ (for asexual parasites), $P_G(a,t)\delta_p\Delta t$ (for sexually committed parasites) and $G(t)\delta_g\Delta t$ (for gametocytes), where δ_p is the natural death rate of parasites and δ_g is the natural death rate of gametocytes. Compartments with a dashed boundary represent those for which parasites of a particular age are sequestered to tissues and thus not measurable by sampling peripheral blood.

following equation:

$$P(a,t) = \begin{cases} P(a-1,t-1) - D_{a-1}, & a = 2,3,\ldots,a_{s-1},a_{s+1},\ldots,a_L \\ r_p\left[P(a_L,t-1) - D_{a_L}\right], & a = 1 \end{cases} \tag{1}$$

where a_L is the duration (in hours) of each asexual replication cycle, a_s is the age at which sexual commitment occurs, r_p is the parasite replication rate and D_a represents the number of dead asexual parasites in age bin a during each time step (one hour), sampled from a Poisson distribution $\mathrm{Poi}(P(a-1,t-1)\delta_p\Delta t)$, where δ_p is the rate of natural death of asexual parasites. For those parasites that may undergo sexual

commitment (i.e., parasites with age a_s):

$$\begin{cases} P(a_s+1,t) = P(a_s,t-1) - D_{a_s} - B, \\ P_G(a_s+1,t) = B, \end{cases} \tag{2}$$

where B represents the number of parasites that become sexually-committed, sampled from a binomial distribution $\mathrm{Bin}(P(a_s,t-1)-D_{a_s},f)$ where f is the probability of sexual commitment for each parasite. The first line of Eq. 2 captures the evolution of the parasites remaining in the asexual life cycle, while the second line of Eq. 2 describes the number of parasites undergoing sexual commitment. Sexually committed parasites continue the rest of the replication cycle, which is modeled by:

$$P_G(a,t) = \begin{cases} P_G(a-1,t-1) - D_{P_G,a-1}, & a = 2,3,...,a_{s-1},a_{s+1},...,a_L \\ r_p\left[P_G(a_L,t-1) - D_{P_G,a_L}\right], & a = 1 \end{cases} \tag{3}$$

where $D_{P_G,a}$ represents the number of dead sexually-committed parasites for age bin a in each time step (one hour), sampled from $\mathrm{Poi}(P_G(a,t-1)\delta_p\Delta t)$. The sexually committed parasites will develop into immature gametocyte stages (i.e., G_1–G_4) and eventually mature male gametocytes G_M and female gametocytes G_F, both of which circulate in the bloodstream. The dynamics of the gametocytes G_1-G_4 are modeled by:

$$\begin{cases} G_1(t) = P_G(a_s-1,t-1) - D_{P_G,a_s-1} + G_1(t-1) - D_{G_1} - M_{1\,to\,2}, \\ G_i(t) = G_i(t-1) + M_{i-1\,to\,i} - D_{G_i} - M_{i\,to\,i+1}, \quad i = 2,3,4 \end{cases} \tag{4}$$

where D_{G_i} represents the number of dead stage i gametocytes, sampled from $\mathrm{Poi}(G_i(t-1)\delta_g\Delta t)$, where δ_g is the death rate of immature gametocytes and $M_{i\,to\,i+1}$ represents the number of stage i gametocytes maturing to become stage $i+1$ gametocytes, sampled from $\mathrm{Poi}(G_i(t-1)m\Delta t)$ for $i = 1,2,3,4$, where m is the rate of gametocyte maturation. Male and female gametocytes develop after stage IV [2] and their dynamics are modeled by:

$$\begin{cases} G_M(t) = G_M(t-1) - D_M + B_M, \\ G_F(t) = G_F(t-1) - D_F + B_F, \end{cases} \tag{5}$$

where D_M represents the number of dying male gametocytes during a time step, sampled from $\mathrm{Poi}(G_M(t-1)\delta_{gc})$, where δ_{gc} is the death rate of circulating gametocytes. Similarly, D_F represents the number of dying female gametocytes during a time step, sampled from $\mathrm{Poi}(G_F(t-1)\delta_{gc})$, B_M represents the num-

ber of immature gametocytes that become male gametocytes, sampled from $\text{Bin}(M_{4to5}, f_G)$, where f_G is the probability that a sequestered G_4 gametocyte develops into a male gametocyte and B_F represents the number of immature gametocytes that become female gametocytes, given by $M_{4to5} - B_M$.

2.1.2 Human-to-mosquito transmission

To model human-to-mosquito transmission, we extend the within-mosquito model developed in [17] to include a probabilistic component to capture the process of gametocyte transmission from human to mosquito. Our model captures the stages of the lifecycle within the mosquito from gametocytes into oocysts and sporozoites, each of which are important developmental stages of the malaria parasite in the mosquito. Following [17], transition times from a pre-oocyst parasite stage (which is explicitly modeled as zygotes in our model) to oocysts and from oocysts to sporozoites are modeled, and the model does not include any outflow due to the death of parasites within the mosquito during the development process from zygotes to sporozoites. The oocyst or sporozoite counts are the target development stage for measurement in mosquito feeding assays [27–29]. Fig 2 presents a schematic diagram of the model, describing the uptake of gametocytes by a mosquito and their development into sporozoites.

The number of male gametocytes taken by a mosquito during a blood meal, M, is assumed to follow the binomial distribution:

$$M \sim \text{Bin}(G_M f_e, p_u), \tag{6}$$

where f_e is the fraction of the total human blood volume V_H localized to the site of a mosquito bite. The total number of male gametocytes available for mosquito uptake in a blood meal is given by $G_M f_e$, based on the assumption that circulating male gametocytes are homogeneously distributed throughout the blood. The probability of gametocyte uptake by the mosquito, p_u, is given by $p_u = V/(f_e V_H)$, which is the ratio of a mosquito blood meal volume V to the volume of blood $f_e V_H$ that contains $G_M f_e$ male gametocytes. Note that f_e has an upper bound of 1 based on its definition and a lower bound of V/V_H below which the selection probability p_u becomes 1 and the binomial distribution model is no longer valid to capture the biological process. The number of female gametocytes taken by a mosquito during a blood meal F is similarly defined as follows:

$$F \sim \text{Bin}(G_F f_e, p_u). \tag{7}$$

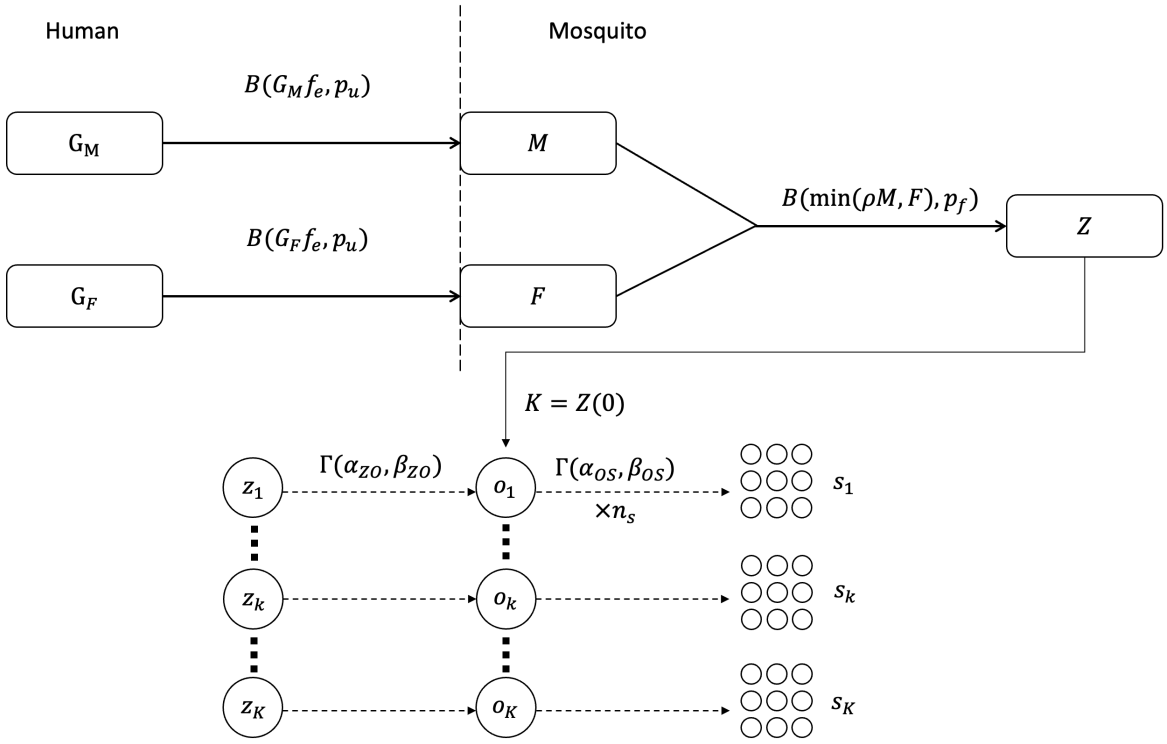

Figure 2: **Human-to-mosquito transmission model.** M and F represent the number of male and female gametocytes taken by a single mosquito during a blood meal, sampled from a binomial distribution $\text{Bin}(G_{\{M,F\}} f_e, p_u)$, where G_M and G_F are the number of male and female gametocytes in the bitten human, f_e is the fraction of the total human blood volume V_H localized to the site of a mosquito bite (V_H is assumed to be 4000mL), and p_u is the probability of uptake by the mosquito, which is the ratio of a mosquito blood meal volume V to the volume of blood $f_e V_H$. Z represents the number of zygotes. The initial number of zygotes $Z(\tau = 0)$ is sampled from a binomial distribution $\text{Bin}(\min(\rho M, F), p_f)$, where ρ is the male gamete-to-gametocyte ratio, defined as the product of the fraction of male gametocytes that are able to produce male gametes via meiosis p_g and the number of male gametes that are produced by male gametocytes and viable for fertilization α, and p_f is the probability of successful fertilization for each pair of gametes. Each zygote z_k ($k \in \{1, 2, \ldots, K\}$, $K = Z(0)$) develops into an oocyst o_k with a transition time sampled from a gamma distribution $\Gamma(\alpha_{ZO}, \beta_{ZO})$. Each oocyst o_k then produces n_s salivary gland sporozoites s_k after an additional time sampled from a gamma distribution $\Gamma(\alpha_{OS}, \beta_{OS})$. Each oocyst produces n_s salivary gland sporozoites.

After ingestion, gametocytes develop into gametes and undergo fertilization to form zygotes which will develop into oocysts [30]. A female gametocyte only becomes a single female gamete while a male gametocyte produces a small number of male gametes via a replication process [20, 21, 31]. However, not all male gametocytes ingested by mosquitoes undergo replication to produce male gametes [32], and some of the male gametes lack nuclei and are therefore not viable for fertilization [21]. Accordingly, the initial number of zygotes $Z(\tau = 0)$ is modeled by a binomial distribution:

$$Z(\tau = 0) \sim \text{Bin}(\min(p_g \alpha M, F), p_f), \tag{8}$$

where p_g is the fraction of male gametocytes that are able to produce male gametes via replication, α is the number of male gametes that are produced by male gametocytes and viable for fertilization and p_f is the probability of successful fertilization. Since p_g and α are structurally non-identifiable, we define $\rho = p_g\alpha$, which represents the ratio of the number of viable male gametes to the number of male gametocytes ingested by the mosquito (henceforth referred to as the *male gamete-to-gametocyte ratio*). After determining the initial number of zygotes $Z(\tau = 0)$ post feeding, for each of the zygotes z_k ($k \in \{1, 2, ..., N\}$, $K = Z(0)$), the process of the development from zygote to oocyst O and subsequently sporozoite S is modeled using an individual based model. For each zygote z_k, transition times are sampled by randomly generating the transition times individually. The number of oocysts $O(\tau)$ and sporozoites $S(\tau)$ at time τ post feeding are modeled by:

$$O(\tau) = \Sigma_{k=1}^{K} \Phi_O(k, \tau), \tag{9}$$

where

$$\Phi_O(k, \tau) = \begin{cases} 1, & \tau'_k \leq \tau < \tau'_k + \tau''_k \\ 0, & otherwise \end{cases}, \tag{10}$$

and

$$S(\tau) = n_s \Sigma_{k=1}^{K} \Phi_S(k, \tau), \tag{11}$$

where

$$\Phi_S(k, \tau) = \begin{cases} 1, & \tau \geq \tau'_k + \tau''_k \\ 0, & otherwise \end{cases}. \tag{12}$$

In Eqs. 10 and 12, τ'_k is the transition time from Z to O for the kth zygote, sampled from a gamma distribution $\Gamma(\alpha_{ZO}, \beta_{ZO})$, τ''_k is the transition time from O to S for the kth zygote, sampled from a gamma distribution $\Gamma(\alpha_{OS}, \beta_{OS})$, where α_{ZO} and α_{OS} are the shape parameters and β_{ZO} and β_{OS} are the rate parameters of the gamma distributions and n_s is the number of salivary gland sporozoites produced per oocyst. As our focus (and data) is on the process of human-to-mosquito infection, rather than on the subsequent infectiousness of the mosquito back to humans, we compute indicator functions for the

infected status of the mosquito:

$$\mathbf{1}_O(\tau) = \begin{cases} 1, & O(\tau) > 0 \\ 0, & O(\tau) = 0 \end{cases}, \tag{13}$$

and

$$\mathbf{1}_S(\tau) = \begin{cases} 1, & S(\tau) > 0 \\ 0, & S(\tau) = 0 \end{cases}. \tag{14}$$

We adopt the same parameter values of distributions of state transitions as those in [17] to determine the times of transition of a zygote into oocysts and then sporozoites. However, Stopard et al. [17] did not include a multiplication factor n_s from stage O to S for the sporogony process whereby a single oocyte produces a large amount of sporozoites. By including n_s in our model, computation of the number of sporozoites within a mosquito will be more biologically accurate (with likely implications for mosquito-to-human transmission).

2.2 Mosquito feeding assays and the human-to-mosquito transmission probability

We consider a single infected human, with male and female gametocytes G_M and G_F circulating in their bloodstream, and a feeding assay in which N_M mosquitoes are brought into contact with that infected human host. Assuming the gametocyte concentration in the human bloodstream does not vary over the time during which the N_M mosquitoes take their blood meals, we model the number of male and female gametocytes ingested by each of the N_M mosquitoes using Eqs. 6–7. For each mosquito, we use Eq. 8 to calculate the initial number of zygotes $Z(0)$. The mosquito is considered to be infected if it has at least one zygote $Z(0) \geq 1$ (which is equivalent to having at least one oocyst given our model assumption that all the zygotes will develop into oocysts). We then simulate Eqs. 9–14 for each of the infected mosquitoes to compute the presence of oocysts and sporozoites post feeding. Mosquitoes may die during the mosquito feeding assay. To account for the effect of mosquito infection status on mosquito death, we assume the mosquito death rate μ_M to be a Gompertz function of time τ, where the parameters governing the Gompertz function are estimated using experimental data provided in [17] (details about the function and data fitting are provided in the S1 Appendix). The time of death t'_n for the nth mosquito is determined by solving

$$p'_n = e^{\int_0^{t'_n} \mu_M(\tau) d\tau} \tag{15}$$

for t'_n where p'_n is a random number sampled from a uniform distribution $U[0,1]$. After we compute the death time for each of the N_M mosquitoes, we model whether the nth mosquito survives for a duration τ post feeding using:

$$L_n(\tau) = \begin{cases} 1, & \text{if } t'_n > \tau \\ 0, & \text{otherwise} \end{cases}. \tag{16}$$

With the mortality status of each of the mosquitoes determined, we calculate the proportion of surviving mosquitoes with developed oocysts (P_e):

$$P_e = \frac{\sum_{n=1}^{N_M} \mathbf{1}_{O,n}(\tau = 8.5) L_n(\tau = 8.5)}{\sum_{n=1}^{N_M} L_n(\tau = 8.5)}, \tag{17}$$

where the choice of $\tau = 8.5$ days is based on the detection time of oocysts in the VIS data [24]. P_e will be fitted to the direct feeding assay data in the VIS [24] to estimate several biological parameters, and the details about the data and fitting methods will be provided in the following sections. We also calculate the proportion of surviving mosquitoes with developed sporozoites (P_i):

$$P_i = \frac{\sum_{n=1}^{N_M} \mathbf{1}_{S,n}(\tau = 15) L_n(\tau = 15)}{\sum_{n=1}^{N_M} L_n(\tau = 15)}, \tag{18}$$

where the choice of $\tau = 15$ days is based on the detection time of sporozoites in previous experiments [27, 28]. P_i will be used in model predictions, as only surviving mosquitoes with developed sporozoites are capable of onward transmission to a susceptible human.

2.3 Model parameters

All model parameters are listed in Table 1. The parameter values for the within-human model are chosen from [13]. The value for the fraction of sequestered G_4 gametocytes developing into male gametocytes (f_G) is obtained based on [19]. The value for the blood meal volume taken by a mosquito (V) is obtained based on [33]. For the fraction of total human blood volume localized to the site of a mosquito bite (f_e), the value should be much larger than V/V_H to retain stochasticity in the sampling process while also being much smaller than 1 as a mosquito blood meal is a localized event and cannot capture any gametocyte circulating in the human blood stream with equal probability. We set f_e to be 0.00025 which corresponds to 1mL localized to the site of mosquito bite. We assume the mosquito bite volume is 3.4μL [33]. Note that the expected value for the number of gametocytes taken in the blood meal is independent of f_e and

the variance only very weakly dependent on f_e. Hence our model is highly insensitive to the choice of f_e (see S1 Fig).

The values of the parameters governing the gamma distributions of the transition time between Z to O and O to S (i.e., α_{ZO}, β_{ZO}, α_{OS} and β_{OS}) are chosen from [17]. The value for the number of salivary gland sporozoites per ruptured oocyst n_s is chosen from [34]. Estimates for the mean number of viable male gametes produced per male gametocyte ρ and the probability of successful fertilization for each pair of gametes p_f are not available in the literature, and as described are key parameters that we estimate through our Bayesian inference procedure (see the next sections for details). The death rates of mosquitoes (μ_M) is estimated by fitting a Gompertz function to mosquito survival data (see S1 Appendix).

All the within-human parameters are included in the partial rank correlation coefficient (PRCC) sensitivity analysis, except for the sequestration age of asexual parasites a_s and the length of the replication cycle of asexual parasites a_L. For the within-mosquito parameters, the blood meal volume taken by mosquito V, the male gamete-to-gametocyte ratio ρ, the probability of successful fertilization for each pair of viable gametes p_f and the ratio of female gametocytes to male gametocytes (G_F/G_M) in the blood meal are included in the PRCC sensitivity analysis. The death rate of mosquitoes μ_M, the parameters governing the gamma distributions describing the transition time between Z to O and O to S, α_{ZO}, β_{ZO}, α_{OS} and β_{OS}, the number of salivary gland sporozoites per ruptured oocyst n_s and the time for detecting oocysts or sporozoites post feeding τ are not included.

2.4 Data and methods for estimating biological parameters

To estimate the male gamete-to-gametocyte ratio ρ and the probability of successful fertilization p_f, we fit the human-to-mosquito transmission model (i.e., Eqs. 6–17) to experimental direct feeding assay data from a previously published VIS [24] using an approximate Bayesian computation sequential Monte Carlo (ABC-SMC) algorithm [35]. The data used in the model fitting include the male and female gametocytemia ($G_M f_e$ and $G_F f_e$ in Eqs. 6–7) in 11 volunteers, measured by PfMGET and Pfs25 qRT-PCR respectively and the proportion of mosquitoes developing oocysts (P_e in Eq. 17). The VIS was approved by the QIMR Berghofer Human Research Ethics Committee and registered with `ClinicalTrials.gov` (NCT02431637 and NCT02431650).

In the ABC-SMC method, the posterior distribution is approximated by comparing the distance between simulated and observed data, with parameter samples initially drawn from the prior distribution and then

Table 1: **Details of parameters, descriptions, units, values and references or comments.**

Parameter	Description	Unit	Value	Reference
P_{init}	Inoculation concentration	parasite/mL	0.08	[13]
μ	Mean of the initial age distribution	h	7	[13]
σ	SD of the initial age distribution	h	5.5	[13]
r_p	Replication number	(unitless)	71	[13]
f	Fraction of parasites entering sexual development	(unitless)	0.006	[13]
δ_p	Death rate of asexual and sexual parasites	h^{-1}	0.03	[13]
δ_g	Death rate of sequestered gametocytes	h^{-1}	0.0004	[13]
δ_{gc}	Death rate of circulating gametocytes	h^{-1}	0.007	[13]
m	Maturation rate of gametocytes	h^{-1}	0.02	[13]
f_G	Fraction of sequestered G_4 gametocytes becoming male gametocytes	(unitless)	0.2	[19]
a_s	Sequestration age of asexual parasites	h	25	[13]
a_L	Length of life cycle of asexual parasites	h	42	[13]
f_e	Fraction of total human blood volume localized to the site of a mosquito bite	(unitless)	0.00025	See the main text
V	Blood meal volume taken by mosquito	μL	3.4	[33]
ρ	male gamete-to-gametocyte ratio	(unitless)	0.80	Estimated
p_f	Probability of successful fertilization for each pair of viable gametes	(unitless)	0.029	Estimated
α_{ZO}	Shape parameter of gamma distribution for transition from Z to O	(unitless)	13.6	[17]
β_{ZO}	Rate parameter of gamma distribution for transition from Z to O	(unitless)	2.7	[17]
α_{OS}	Shape parameter of gamma distribution for transition from O to S	(unitless)	17.8	[17]
β_{OS}	Rate parameter of gamma distribution for transition from O to S	(unitless)	2.2	[17]
n_s	Number of salivary gland sporozoites produced per oocyst	(unitless)	4427	[34]
τ	Time for detecting oocysts or sporozoites post feeding	Day	8.5 or 15	[24, 27]
μ_M	The death rate of mosquitoes	Function of time		Estimated

from a sequence of intermediate distributions, progressively refined using sequential Monte Carlo, and with tolerance gradually decreasing over generations [35]. We first define the prior distributions of ρ and p_f. To inform the prior distribution for ρ, we consider that $\rho = p_g\alpha$, where p_g represents the fraction of male gametocytes undergoing replication to produce male gametes and α is the mean number of viable male gametes produced per male gametocytes undergoing replication. There is substantial uncertainty surrounding the value of p_g, with experimental studies reporting values spanning the full range from 0 to 1 [32, 36]. For α, it is known that each male gametocyte undergoing replication gives rise to 8 male gametes [20], but not all of these are viable, as only gametes containing a nucleus are capable of fertiliza-

tion [21]. Given that at least one nucleus is present per gametocyte, we constrain α to be between 1 and 8, reflecting the plausible biological range. Accordingly, we adopt a prior distribution $U[0,1] \times U[1,8]$ for ρ (see S2 Appendix). For p_f, where limited empirical information is available, we also choose a uniform prior distribution $U[0,1]$, allowing the data to inform the posterior distribution. After specifying the prior distributions, we sample the parameters ρ and p_f from prior distributions independently in the first generation of the ABC-SMC algorithm and from the intermediate posterior distributions in subsequent generations. For each parameter sample (ρ, p_f), simulated data $\{P'_{e,1}, \ldots, P'_{e,11}\}$ are generated for the 11 volunteers by using Eqs. 6–17. We then compute the Euclidean distance d, which is a common choice of distance metric (see [37] for details), between the simulated data $\{P'_{e,1}, \ldots, P'_{e,11}\}$ and observed data $\{P_{e,1}, \ldots, P_{e,11}\}$, as follows:

$$d = \left[\sum_{i=1}^{11} \left(P'_{e,i} - P_{e,i} \right)^2 \right]^{1/2}. \tag{19}$$

The sampling process is repeated until 5000 samples are accepted in each generation. The algorithm terminates when the acceptance rate falls below 0.5%, which serves as the stopping rule [38]. Full details of the ABC-SMC implementation, including the choice of tolerance, resampling and weighting, and pseudo-code, are provided in S2 Appendix. After obtaining the fitting results, we report the joint posterior distribution of ρ and p_f (Fig 3).

2.5 Data and code availability

Model analysis and result visualization are performed in R studio (version 4.2.1). All the code, data and fitting results are publicly available at `https://github.com/XSSUN2/Modelling-the-transmission-of-malaria-parasites-from-a-human-host-to-mosquitoes.git`.

3 Results

3.1 The number of viable male gametes and the probability of successful fertilization

Application of our model to the VIS data provides estimates for the male gamete-to-gametocyte ratio ρ, and the probability of successful fertilization p_f (Fig 3). The maximum a posteriori (MAP) estimate (i.e., the value with the highest density in the posterior distribution) for the male gamete-to-gametocyte ratio ρ is 0.80 with a 95% highest density posterior interval (HDPI) of 0.13–2.90. Recall that ρ is the product of the fraction of male gametocytes that are able to produce male gametes via replication p_g and

the number of viable male gametes produced by male gametocytes α and therefore the a priori range for ρ is 0 to 8. The MAP estimate for the probability of successful fertilization p_f is 2.90% (95% HDPI: 0.57–10.92%). Note that the samples of the posterior distribution exhibit a negative correlation between ρ and p_f (i.e. the hyperbolic shape of the density scatter plot in Fig 3), suggesting that the available data are insufficient to distinguish between explanations in which a high true value for ρ corresponds to a low true value for p_f, and vice versa.

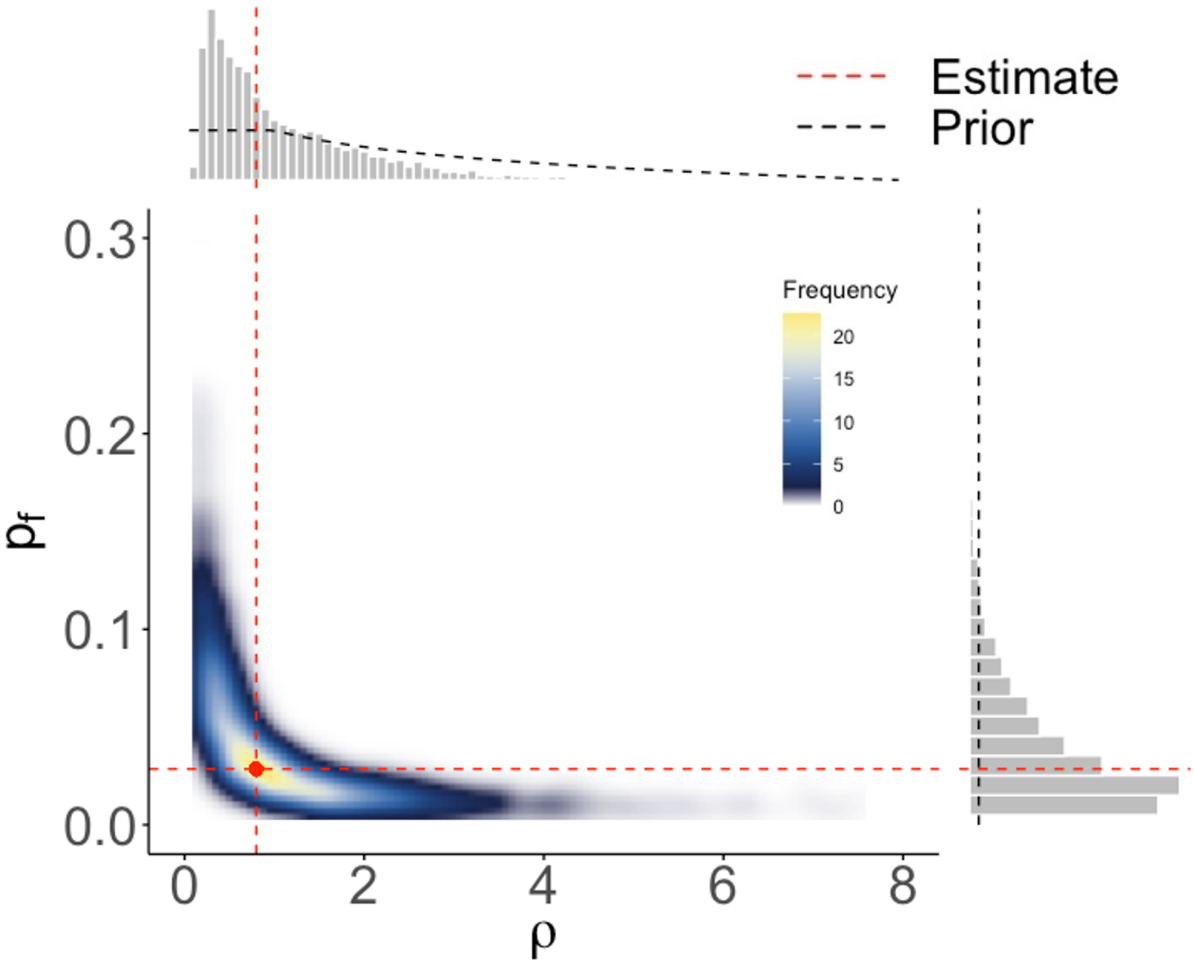

Figure 3: **Estimation results for parameters governing viability of male gametes and fertilization.** The figure displays the joint and marginal distributions of 5,000 posterior samples for the male gamete-to-gametocyte ratio (ρ) and the probability of successful fertilization per gamete pair (p_f). Black dashed curves indicate the prior distributions of the parameters. The red lines intersect at the maximum a posteriori (MAP) estimates (the point with the highest posterior density).

3.2 Human and mosquito factors that most strongly influence the probability of human-to-mosquito transmission

We first examine how the within-human parameters affect the level of gametocytemia. To identify model parameters that most strongly influence the development of gametocytes, we perform a partial rank correlation coefficient (PRCC) analysis [39] (Fig 4). In detail, we generate 1000 sets of within-human model parameters by sampling from the joint uniform distribution where the range of each parameter is set to be ±50% of its benchmark value (as per Table 1). We then calculate the time, t_G, at which an individual's gametocytemia reaches 10^3 parasites/mL blood (a threshold below which human-to-mosquito transmission is not observed [24]) for each of the 1000 parameter sets using the within-human parasite dynamics model (i.e., Eqs. 1-5).

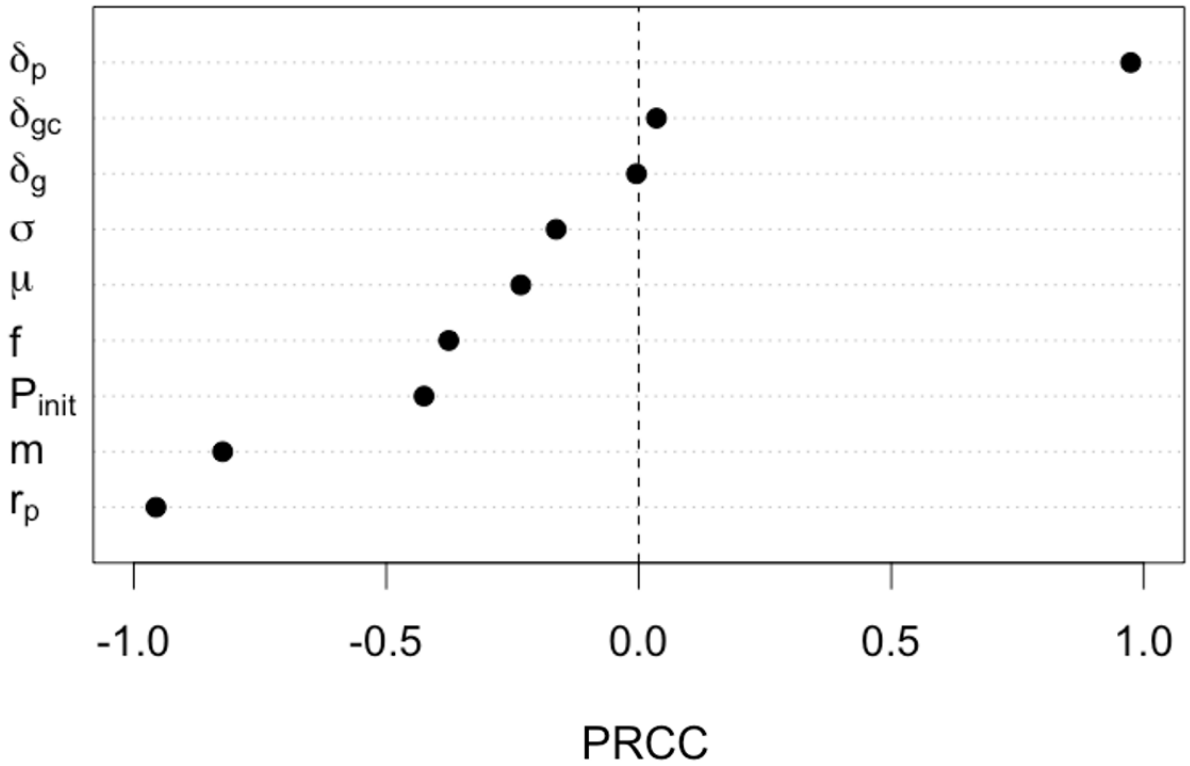

Figure 4: **PRCC results between parameters and t_G.** The top three parameters that influence the t_G (i.e., those with the largest absolute values) are δ_p (PRCC=0.97), r_p (PRCC=-0.96), and m (PRCC=-0.82).

The three parameters that are most highly correlated with t_G are the death rate of parasites δ_p, the parasite replication number r_p, and the maturation rate of gametocytes m. The first two factors are closely related to the multiplication factor of asexual parasites [13], and the third quantifies the delay between gametocytes maturation and circulation in the blood. Relaxing the range over which the parameters are

sampled in the PRCC analysis from ±50% of their benchmark values to ±75% in the PRCC analysis does not alter the findings (see S2 Fig).

We now examine how the parameters that most strongly influence t_G (i.e., δ_p, r_p and m) affect the time series curve for the gametocytemia. As expected from the PRCC analysis, increasing δ_p slows the gametocyte development t_G (Fig 5A). Likewise, increasing r_p and m accelerates the gametocyte development t_G (Figs 5B and C).

We also examine how the gametocyte development depends on the sexual commitment rate f, which is an important biological parameter modulating the number of parasites that develop into gametocytes and in turn influencing the probability of malaria transmission from human to mosquito [40]. Fig 6 shows that increasing the sexual commitment rate f increases the level of gametocytemia and reduces the time to reach a certain level of gametocytemia, (e.g., 10^3 used to calculate t_G), which is consistent with the negative correlation between f and t_G in the PRCC analysis (Fig 4). The right panel of Fig. 6 suggests that the dependence of t_G on f exhibits an exponential-like relationship, such that a more significant change in gametocytemia occur when f is relatively small (e.g., less than 0.02) compared to when f is large (e.g., larger than 0.05).

Having examined how the within-human parameters affect the level of gametocytemia, we now examine how mosquito parameters affect the probability of human-to-mosquito transmission. As above, we conduct a PRCC analysis to examine the relative contributions of different model parameters to the probability of human-to-mosquito transmission. We generate 1000 sets of parameter values by sampling from the joint uniform distribution of four parameters V, ρ, p_f and the ratio of female gametocytes to male gametocytes G_F/G_M. The range of each parameter is set to be ±50% of its benchmark value (i.e., $V = 3.4$ are taken from [33], $\rho = 0.80$ and $p_f = 0.029$ are estimated and $G_F/G_M = 4$ is taken from [19]). For each of the 1000 parameter sets and a given level of gametocytemia G (taken to be $G = 10^3$, 10^4 or 10^5 per ml blood, noting that the transmission probability saturates when G is high), we use our human-to-mosquito transmission model to compute the probability of human-to-mosquito transmission P_i (Eqs. 6–18).

The PRCC analysis (Fig 7A) shows that the most influential factors positively correlated with the transmission probability P_i are the blood volume V taken by a mosquito, the probability of successful fertilization p_f and the male gamete-to-gametocyte ratio ρ. The ratio of female to male gametocytes G_F/G_M is negatively correlated with the transmission probability P_i for all three gametocytemia levels examined. Relaxing the range of parameters from ±50% of their benchmark values to ±75% in the PRCC analysis

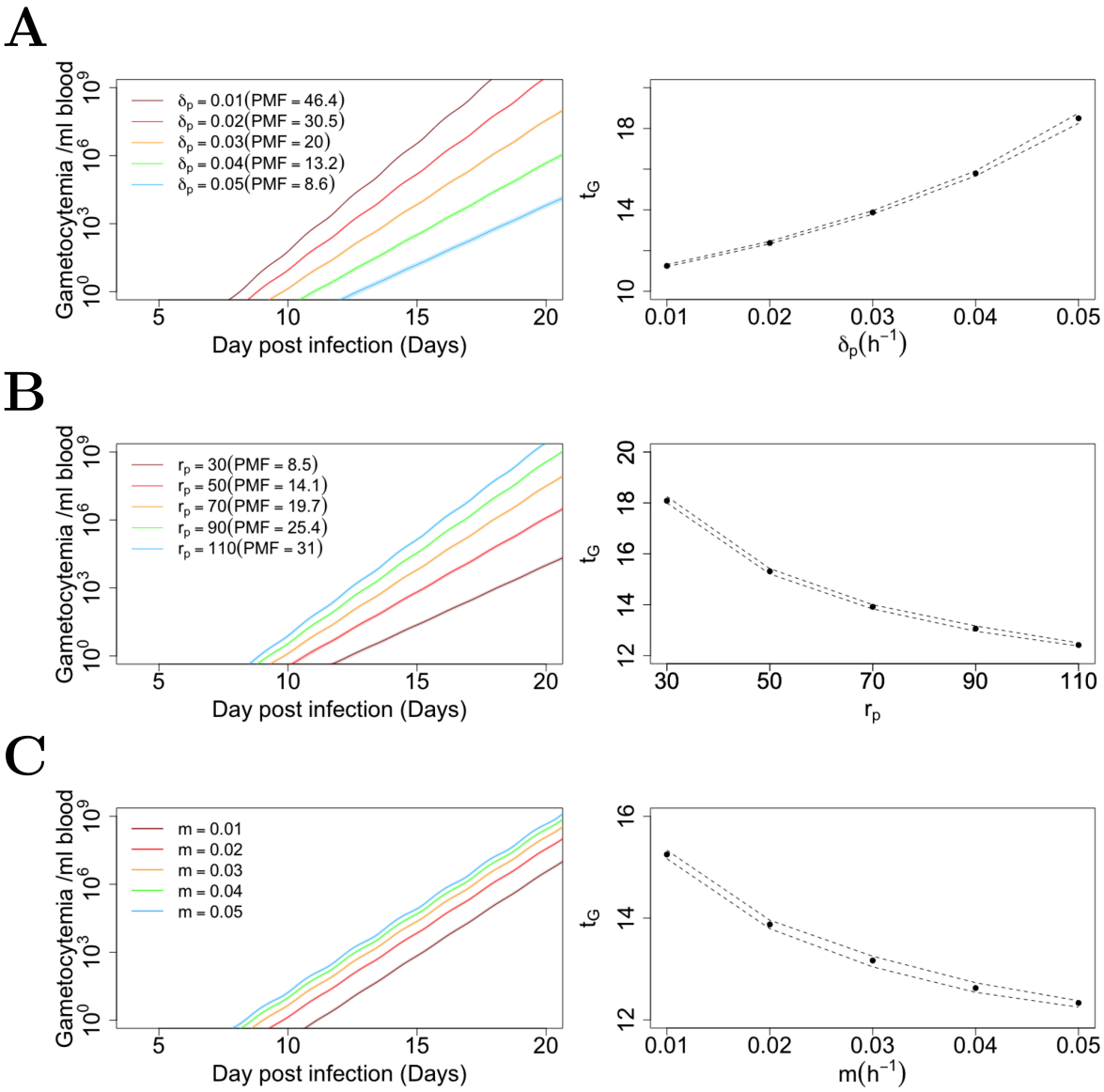

Figure 5: **Sensitivity analysis for δ_p, r_p and m.** (A) The time series of gametocytemia for different values of δ_p (left), and the relationship between t_G and δp (right). (B) The time series of gametocytemia for different values of r_p (left), and the relationship between t_G and r_p (right). (C) The time series of gametocytemia for different values of m (left), and the relationship between t_G and m (right). For the time series of gametocytemia, median predictions are represented by solid lines, and 95% prediction intervals (PI) are represented by shaded areas. For t_G, median predictions are represented by dots, and 95% PIs are represented by dashed lines.

does not alter the conclusions (see S3 Fig). Fig 7B–E show that an increase in gametocytemia from 10^3 to 10^5 leads to a higher human-to-mosquito transmission probability, as well as an increase in the range that P_i would reach. This trend is similar to the findings in [41], where a decrease in gametocyte density due to drug administration reduces both the median and the range of the probability of transmission in mosquito feeding assays.

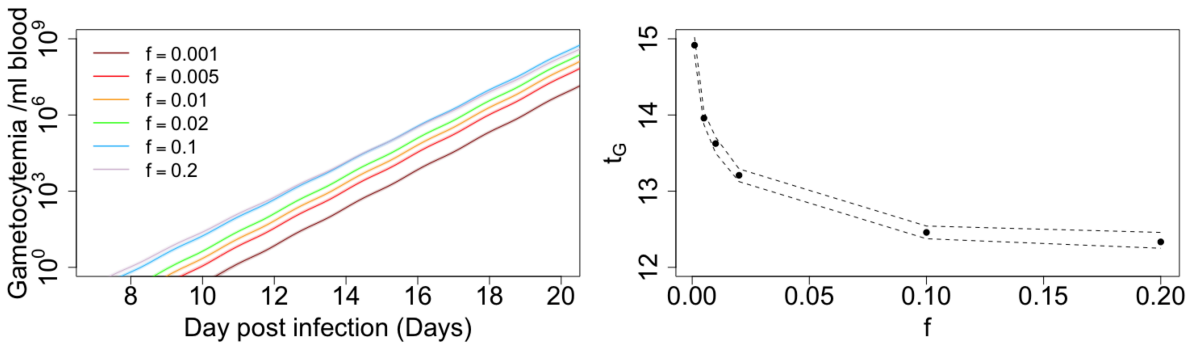

Figure 6: **Sensitivity analysis for f.** The time series of gametocytemia for different values of f (left), and the relationship between t_G and f (right). For the time series of gametocytemia, median predictions are represented by solid lines, and 95% prediction intervals (PI) are represented by shaded areas. For t_G, median predictions are represented by dots, and 95% PIs are represented by dashed lines. Note that the time series of gametocytemia overlap for $f = 0.1$ and 0.2 (i.e., doubling f from 0.1 to 0.2 does not materially change the time series).

3.3 Asexual parasitemia's influence on the probability of human-to-mosquito transmission

While the sensitivity analyses report above quantify how different human and mosquito host factors influence the probability of human-to-mosquito transmission, they do not provide the information necessary to establish a direct relationship between the parasitemia (i.e., asexual parasites per ml of blood) in an infected human and the probability of transmission. Establishing this relationship is of central importance as asexual parasitemia is the primary indicator for diagnosis and surveillance, and knowledge of how it influences the probability of human-to-mosquito transmission is critical for evaluating the likely impact of clinical and public health control measures against malaria. Some field studies have shown that asymptomatic infections generally have lower parasitemia in low transmission settings (approximately 10^4 parasites/mL blood) [5, 42, 43], compared to those in high transmission settings (approximately 10^6 parasites/mL blood) [5, 43–45]. To identify the relationship between the parasitemia informed by the field studies and the transmission probability, we extend our within-human model to include a time-dependence on the parasite multiplication rate r_p. This allows us to simulate an individual who, following exposure and a period of exponential growth in asexual parasitemia, reaches a state in which the mean parasitemia level (over the natural life cycle) is cyclical at a set-point level (e.g., 10^4, 10^5, 10^6 and 10^7, see Fig 8A for example) and the gametocytemia level reaches a steady level (Fig 8B). This time-dependence on r_p allows us to simulate the phase of asymptomatic infection in which the immune response is active, yielding a cyclical asexual parasitemia at a set-point level. For asymptomatic infection with a set-point parasitemia level of 10^4 parasites/mL, the human-to-mosquito transmission probability P_i is negligible.

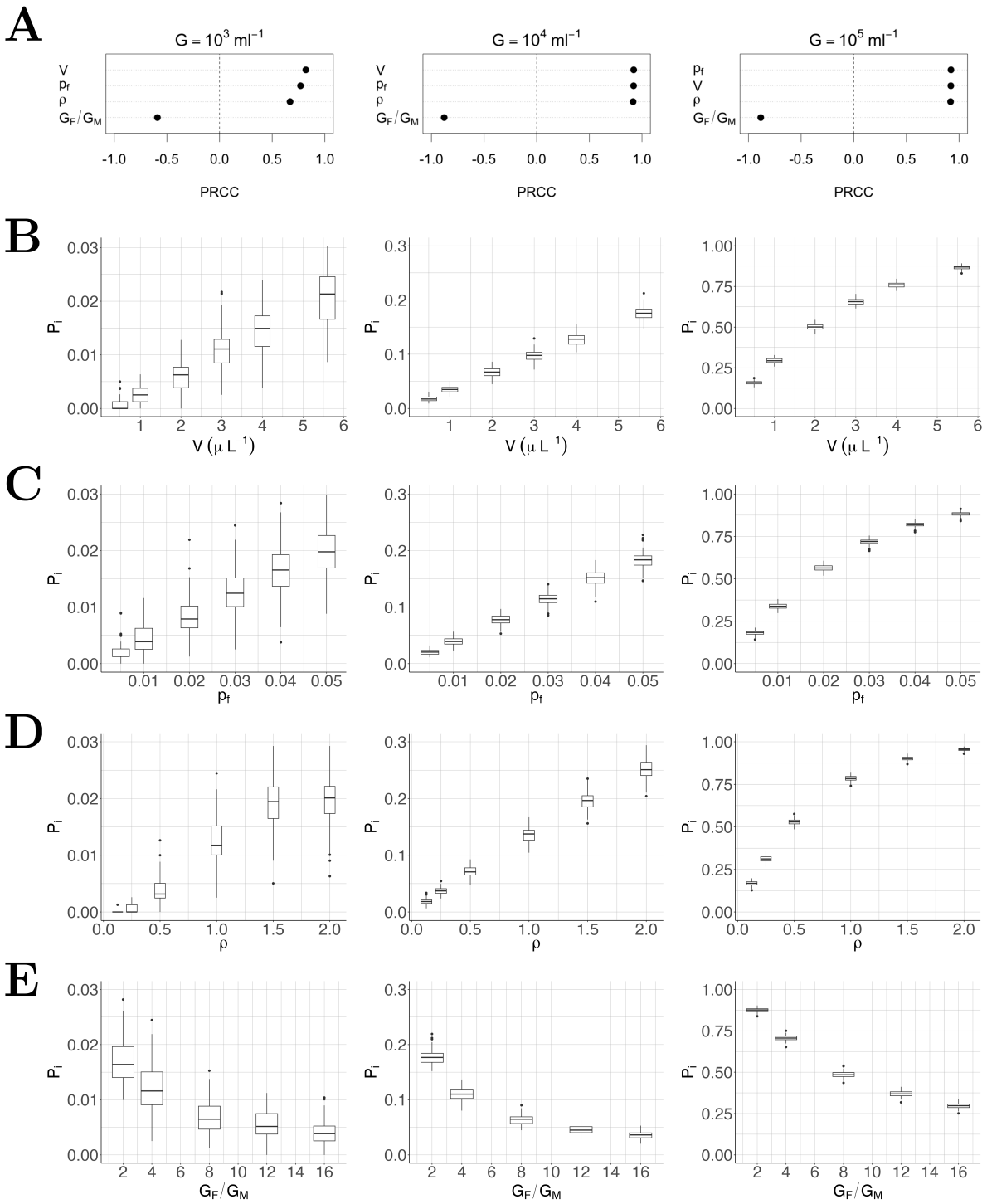

Figure 7: **PRCC results between mosquito parameters and P_i and sensitivity analysis for V, p_f, ρ and G_F/G_M at different gametocytemia level (10^3, 10^4 and 10^5).** (A) PRCC values for the parameters. (B) The relationship between P_i and V. (C) The relationship between P_i and p_f. (D) The relationship between P_i and ρ. (E) The relationship between P_i and G_F/G_M. To calculate the transmission probability P_i, 1000 mosquito feeding assays with $N_M = 1000$ mosquitoes in each assay are simulated using Eqs. 6-18.

For parasitemia levels beyond 10^6 parasites/mL, the human-to-mosquito transmission probability P_i increases rapidly, and for parasitemia levels beyond 10^7 parasites/mL, P_i reaches near 100% (Fig 8C and D). As our model computes the number of salivary gland sporozoites, we also examine the relationship between the set-point asexual parasitemia level and the sporozoite count. We find that higher parasitemia is associated with a higher number of sporozoites developing in the mosquitoes (Fig 9 and S4 Fig).

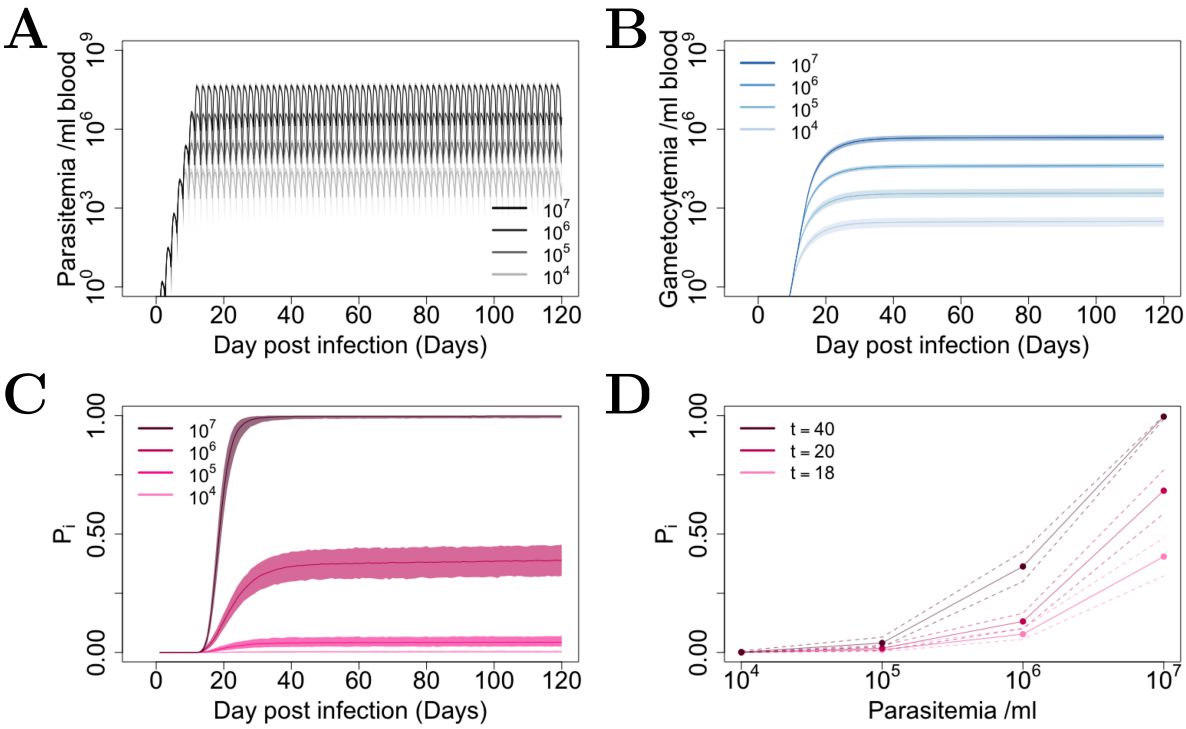

Figure 8: **The relationship between the probability of human-to-mosquito transmission P_i per mosquito blood meal and parasitemia level.** The figure shows the simulations of asexual parasitemia of humans with asymptomatic infection around 10^4, 10^5, 10^6 and 10^7 (A), the corresponding gametocytemia (B) and the corresponding probability of human-to-mosquito transmission P_i (C), which are represented by colors from light to deep. The median predictions are represented by solid lines, and the 95% PIs are represented by shaded areas. (D) shows the relationship between parasitemia level and P_i at three time points (day 18, 20 and 40 post infection). To calculate the median and 95% PIs, 1000 humans with asymptomatic infection are simulated for different parasitemia levels, with 1000 mosquitoes simulated to feed on each human to calculate the probability of human-to-mosquito transmission P_i.

4 Discussion

In this study, we have developed a multi-scale model of human-to-mosquito malaria transmission, combining parasite dynamics in both humans and mosquitoes. Through application to experimental data, we have used the model to estimate several biological parameters, thereby quantifying the effect of various human and mosquito factors on the probability of human-to-mosquito transmission. Our primary find-

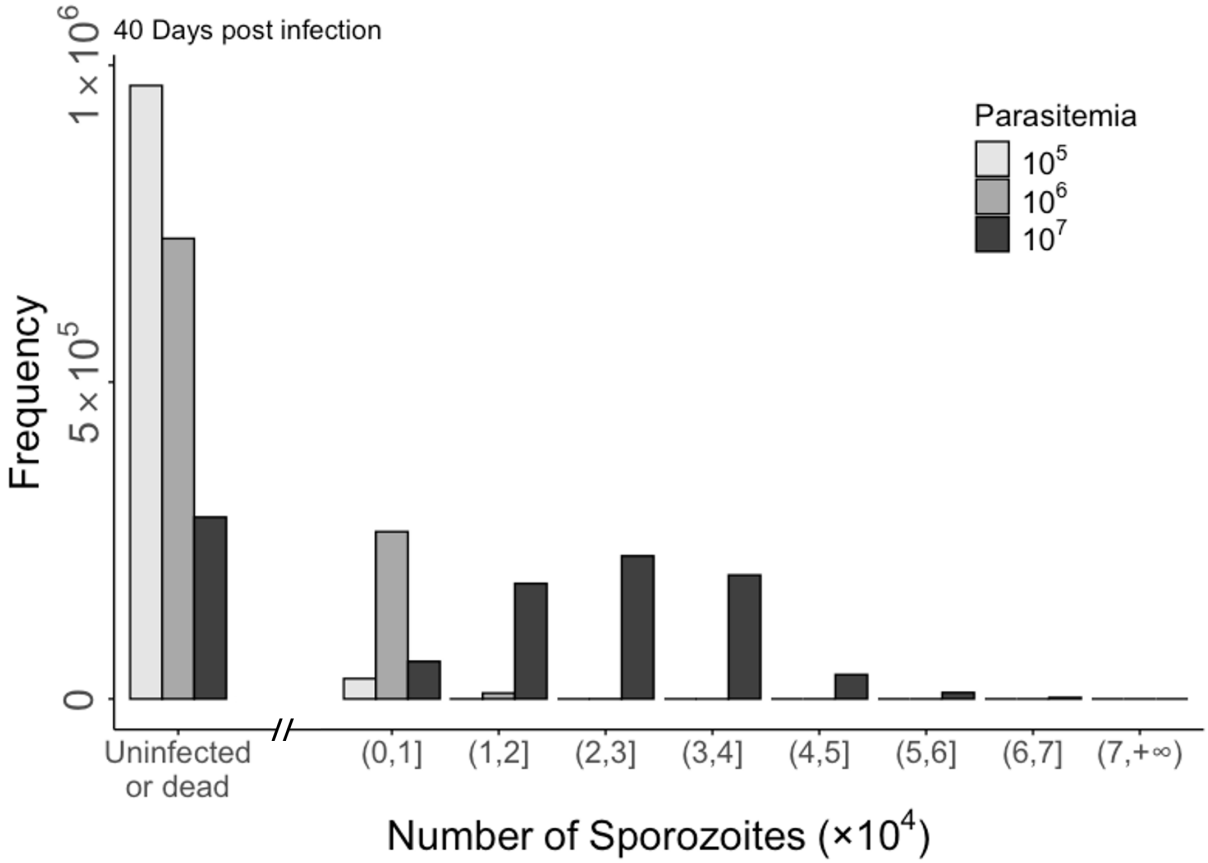

Figure 9: **Distributions of salivary gland sporozoites per blood meal in mosquitoes after feeding on humans with asymptomatic infection.** The relationship between parasitemia level (10^5, 10^6 and 10^7) and the number of sporozoites in mosquitoes ($S(\tau = 15)$ in Eq. 11) at 40 days post infection. To generate the distributions, 1000 humans with asymptomatic infection are simulated for different parasitemia levels, with 1000 mosquitoes simulated to feed on each human. That is, for each of the parasitemia levels, 10^6 samples are allocated into different groups based on the status of the mosquito (uninfected or dead) or the number of sporozoites in the mosquito.

ings include: (1) estimation of two key biological parameters, the ratio of the number of viable male gametes to the number of male gametocytes ρ (per mosquito blood meal), and the probability of successful fertilization of a female and a male gamete p_f; and (2) identification of the relative contributions of different host factors on the probability of human-to-mosquito transmission; and (3) quantification of the effect of the level of asexual parasitemia on the probability of human-to-mosquito transmission. Our work provides the first comprehensive quantitative understanding of the biological processes underpinning the transmission of malaria parasites from human hosts to mosquitoes. Furthermore, it provides a data-analytic framework that integrates mathematical models, human challenge data and statistical inference to study malaria infection and transmission.

We have estimated ρ to be 0.80 (95% HDPI: 0.13–2.90). By definition, ρ is an aggregate quantity rep-

resenting the product of two biological parameters: the fraction of male gametocytes that are able to produce male gametes via replication p_g and the number of male gametes that are produced by male gametocytes and viable for fertilization α. Our estimate of ρ suggests that the number of viable male gametes developing within a mosquito is approximately 80% of the total number of male gametocytes taken in a blood meal. However, the available data do not allow us to determine the two biological factors that combine multiplicatively to produce ρ. Additional experimental studies may provide direct estimation of one or both of p_g and α. For example, it is known that each male gametocyte undergoing meiosis can produce eight gametes [20], but approximately 40% or fewer of the resultant male gametes have a nucleus and are therefore permissive of fertilization [21], suggesting α is likely to be less than four for the cited experimental studies. Furthermore, there is a large uncertainty in the fraction of male gametocytes undergoing meiosis to produce gametes, with experimental studies reporting values spanning the full range from 0 to 1 [32,36]. Our estimate for the probability of successful fertilization p_f between a viable female and a viable male gamete is 2.90% (95% HDPI: 0.57–10.92%), suggesting that only a small proportion of viable gamete pairs can result in successful fertilization. To the best of our knowledge, there have not been any experimental, nor modeling studies yielding an *in vivo* estimate of the fertilization rate, and our work therefore provides the first quantification of the fertilization process through fitting a mathematical model to human challenge data using Bayesian statistical approaches. However, the available data are insufficient to fully determine uncorrelated posterior estimates for ρ and p_f (Fig 3). Future experimental data, particularly the measurement of oocyst counts in mosquitoes post feeding, may help resolve this uncertainty and provide improved (uncorrelated and more precise) estimates of these two parameters.

The sexual conversion rate f is an important parameter driving the kinetics of gametocytemia. In previous studies, it has been shown that this is influenced by a number of factors, including immunity and exposure to antimalarials. This suggests that such factors may have nonlinear influences on transmission [46–48]. For example, some evidence suggests that genetic polymorphisms associated with the development of artemisinin resistance may increase the sexual conversion rate and thus result in increased transmission efficiency. Our analyses provide a quantitative evaluation of this potential effect. The relationship between the sexual conversion rate f and the gametocytemia is strongly nonlinear, but notably has the strongest influence on the timing of likely transmission within the range of predicted values for f provided in [13].

In previous studies, it has likewise been shown that the proportion of mosquitoes infected in mosquito

feeding experiments is positively correlated with the level of gametocytes. However, the variance in the proportion is usually large [6–8]. For example, the proportion of infected mosquitoes can vary from 0% to approximately 70% when the level of gametocytes is between 10^4/mL and 10^5/mL [8]. Our sensitivity analyses in Fig. 7 show that the probability of transmission (which is equivalent to the proportion of infected mosquitoes by definition) can vary from approximately 0–30% for 10^4 gametocytemia/mL to approximately 20–90% for 10^5 gametocytemia/mL, providing quantitatively comparable results to the experimental observations. Our results suggest that a sufficiently large variance in with-host parameters can lead to a large variance in the transmission probability, which may explain the observations in the experiments. However, it should be noted that the parameter values used in our analyses were estimated from a single VIS study (and published works), and therefore the ranges of the parameters examined in the sensitivity analyses (in Fig. 7) may overestimate or underestimate the actual variability that may occur in natural infections. In addition, other factors that our model does not capture, such as host immune responses resulting in temporal fluctuations in transmission reducing immunity, may also contribute to the observed variance [49, 50].

Our model mapping human parasite kinetics to human-to-mosquito transmission has been designed so that it can be incorporated into a multi-scale epidemiological transmission model of malaria infection dynamics, and therefore be used to assess the transmission-blocking effect of interventions such as gametocytocidal drugs or transmission blocking vaccines at a population level. Due to the emergence and geographical spread of antimalarial resistance, there is an increasing interest in deploying such interventions to facilitate malaria elimination [51]. For example, primaquine is highly effective against mature gametocytes, and therefore has been advocated as an addion to the standard artemisinin combination therapy, for its transmission blocking effect [41]. Further, the ability of investigational antimalarials to block transmission to mosquitoes is considered a desirable attribute. In addition, there is significant interest in the development of transmission blocking vaccines that would reduce the probability of successful human-mosquito transmission [52]. Our multi-scale modeling framework will allow us to further incorporate more details, such as pharmacokinetic-pharmacodynamic or epidemiological models, to predict the clinical and public health efficacy of these transmission blocking strategies, and provide valuable insights for optimizing and implementing effective public health responses to malaria.

Our study has several limitations. Firstly, We assume a fixed sexual conversion rate when predicting the transmission probability of asymptomatic infections with different levels of parasitemia. However, it has been shown that parasites in low transmission settings tend to invest more in gametocyte production

compared to high transmission settings [53,54]. Furthermore, longitudinal observations suggest that the ratio of parasitemia to gametocytemia can vary over time [55], which could result from changes in the sexual conversion rate. Secondly, the human-to-mosquito transmission model does not include the detailed within-mosquito dynamics following ingestion of a blood meal but prior to the formation of zygotes in the within-mosquito model. Human immune factors including antibodies and complement, as well as factors from the mosquito's immune system, which could potentially impact gamete development, inhibit the successful fertilization of gametes and kill parasites in the mosquito [15,56–58]. Lastly, we do not include parasite death during the sporogony in the model and do not explicitly model the transformation of zygotes into motile ookinetes and their development toward oocyst formation [2]. Incorporating those processes into the existing model framework would provide a more accurate model for making predictions. However, this would require new experimental data measuring these developmental stages to inform those processes and quantify the model parameters governing those processes with model fitting, which is left for future work.

Supporting information

S1 Appendix.

Estimation of death rate of mosquitoes. Previous analyses on mosquito survival have revealed that a Gompertz function provides an excellent fit to data. Mortality rates generally increase with age for mosquitoes [17, 28, 59]. In our model, the death rate μ is assumed to be a Gompertz function of time τ. We allow for a potential difference between infected ($E = 1$) and uninfected ($E = 0$) mosquitoes:

$$\mu_M(\tau) = ae^{b\tau + cE}, \tag{20}$$

where a, b and c are non-zero constants. The mosquito survival $p(\tau)$ is then given by the following differential equation:

$$\frac{dp}{d\tau} = -\mu_m p \tag{21}$$

To solve this, we separate the variables and integrate both sides:

$$\int \frac{1}{p}\, dp = \int -ae^{b\tau + cE}\, d\tau \tag{22}$$

The equation integrates to:

$$\ln p(\tau) = -\frac{a}{b} e^{b\tau + cE} + C$$

Substitute $p(0) = 1$:

$$C = \frac{a}{b} e^{cE}$$

Finally, we get the solution:

$$p(\tau) = e^{-\frac{a}{b} e^{cE} (e^{b\tau} - 1)} \tag{23}$$

We fit this equation to mosquito survival data (at 27°C in [17]) by using nonlinear least squares estimation *nlsLM* in package *minpack.lm* (with default settings) in R (version 4.2.1). Results are shown in the Figure below.

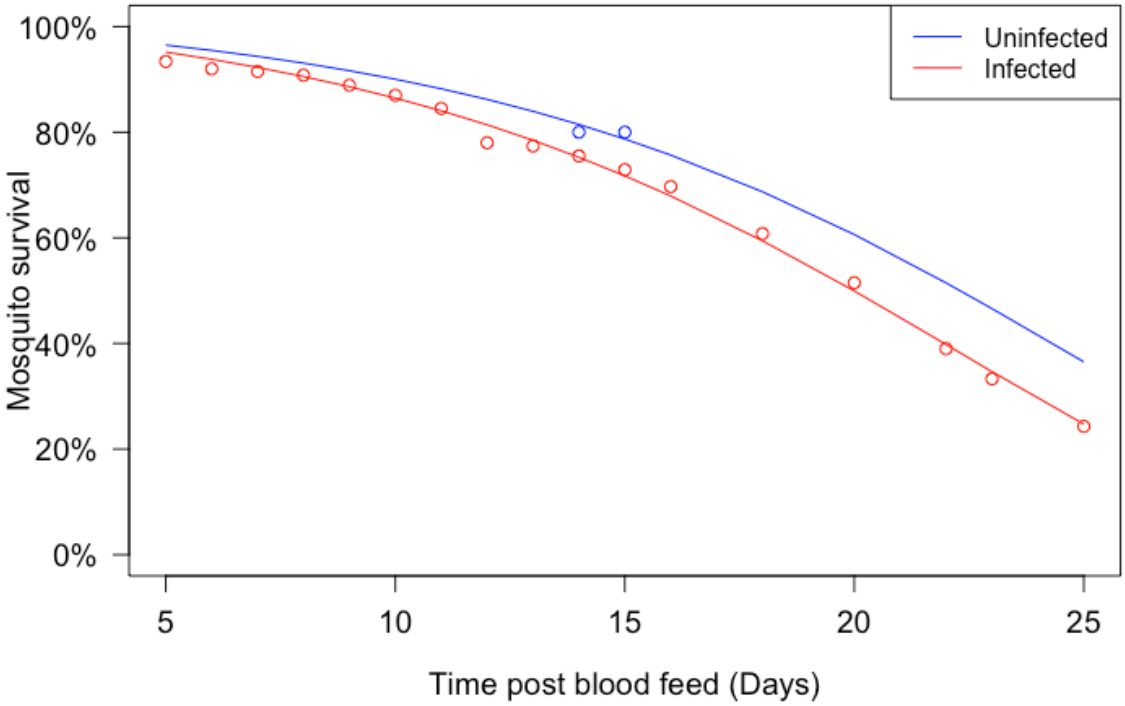

Fitting results for the death rate of mosquitoes μ_M. The dots represent the data for infected mosquitoes (red) and uninfected mosquitoes (blue). The curves are the fitting results for the death rate μ_M (infected $E = 1$, red, and uninfected $E = 0$, blue).

S2 Appendix.

Methods for estimating biological parameters To calculate the density of the prior distribution of ρ, $U[0,1] \times U[1,8]$, we employ the probability density function (PDF) transformation method. Let $X \sim U[0,1]$ and $Y \sim U[1,8]$, and define $Z = XY$. the individual PDFs of X and Y are:

$$f_X(x) = 1, for\ x \in [0,1], \tag{24}$$

$$f_Y(y) = \frac{1}{7}, for\ y \in [1,8]. \tag{25}$$

Since X and Y are independent, the joint PDF of X and Y, denoted by $f_{X,Y}(x,y)$, is:

$$f_{X,Y}(x,y) = f_X(x) f_Y(y) = 1 \times \frac{1}{7} = \frac{1}{7}, for\ x \in [0,1], y \in [1,8]. \tag{26}$$

We are interested in the distribution of $Z = XY$. To derive $f_Z(z)$, we apply the change-of-variable

technique, where the Jacobian determinant is:

$$J = \frac{\partial(z,x)}{\partial(x,y)} = \begin{bmatrix} \frac{\partial z}{\partial x} & \frac{\partial z}{\partial y} \\ \frac{\partial x}{\partial x} & \frac{\partial x}{\partial y} \end{bmatrix} = \begin{bmatrix} y & x \\ 1 & 0 \end{bmatrix} \Rightarrow det(J) = -x. \tag{27}$$

Using this transformation, the PDF of Z is given by:

$$f_Z(z) = \int f_{Z,X}(z,x)dx = \int f_{X,Y}(x,y) \cdot |\frac{\partial(x,y)}{\partial(z,x)}|dx = \int f_{X,Y}(x,y) \cdot |\frac{1}{det(J)}|dx. \tag{28}$$

Since $Y = \frac{z}{x} \in [1,8]$, it follows that $x \in [z/8, min(z,1)]$, and the PDF of Z becomes:

$$f_Z(z) = \int_{x=z/8}^{min(z,1)} f_X(x) f_Y(\frac{z}{x}) \frac{1}{|x|} dx. \tag{29}$$

For $z \in [0,1]$, the PDF is:

$$f_Z(z) = \int_{x=z/8}^{z} \frac{1}{7} \cdot \frac{1}{x} dx = \frac{1}{7} ln8. \tag{30}$$

For $z \in (1,8]$, the PDF is:

$$f_Z(z) = \int_{x=z/8}^{1} \frac{1}{7} \cdot \frac{1}{x} dx = \frac{1}{7} ln(\frac{8}{z}). \tag{31}$$

Therefore, the PDF of Z is:

$$f_Z(z) = \begin{cases} \frac{1}{7} ln8 & z \in [0,1] \\ \\ \frac{1}{7} ln(\frac{8}{z}) & z \in (1,8] \end{cases}. \tag{32}$$

To perform the ABC-SMC, we independently sample the parameters ρ and p_f from prior distributions in the first generation ($g = 1$). For each parameter sample (ρ, p_f), simulated data $\{P'_{e,1}, \ldots, P'_{e,11}\}$ are generated for the 11 volunteers by using Eqs. 6–17. We then compute the Euclidean distance d, which is a common choice of distance metric (see [37] for details), between the simulated data $\{P'_{e,1}, \ldots, P'_{e,11}\}$ and observed data $\{P_{e,1}, \ldots, P_{e,11}\}$, as follows:

$$d = \left[\sum_{i=1}^{11} \left(P'_{e,i} - P_{e,i} \right)^2 \right]^{1/2}. \tag{33}$$

The sampled parameter pairs (ρ, p_f) are accepted in the first generation if $d < \epsilon_1$, where $\epsilon_1 = \sum_{i=1}^{11} (P'_{e,i} - P_{e,i})^2]^{1/2}$ represents the 'data-only' distance. We repeat the sampling process until $L = 5000$ samples $\{(\rho, p_f)_l^{g=1}\}_{l=1}^{L}$ are obtained and assigned an equal normalized weight to each accepted sample

$w_l^{g=1} = 1/L$. For subsequent generations, new samples $(\rho, p_f)^*$ are drawn from the weighted empirical distribution of accepted samples from the previous generation, $\{(\rho, p_f)_l^{g-1}\}_{l=1}^L$, using weights $\{w_l^{g-1}\}_{l=1}^L$. Each sample is perturbed using a multivariate normal kernel $K[(\rho, p_f)|(\rho, p_f)^*]$, with mean and standard deviation set to be the sample mean and standard deviation of the accepted samples from the previous generation $g-1$ to improve sampling efficiency [60]. As in the first generation, simulated data are generated by the model for each perturbed sample (ρ, p_f) and the distance d between the simulated and observed data is calculated. (ρ, p_f) is accepted if $d < \epsilon_g$, where ϵ_g is given by:

$$\epsilon_g = \begin{cases} \left[\sum_{i=1}^{11} \left(P'_{e,i} - P_{e,i}\right)^2\right]^{1/2}, & if\ g = 1 \\ \text{Median}\left(\{d_n^{g-1}\}_{l=1}^L\right), & if\ g = 2, 3, \ldots, G \end{cases}. \tag{34}$$

The process is repeated until $L = 5000$ samples $\{(\rho, p_f)_l^g\}_{l=1}^L$ are accepted in each generation. The weights w^* for accepted samples are calculated using:

$$w^{*g}_k = \begin{cases} 1 & if\ g = 1 \\ \frac{\pi[(\alpha, p_f)_l^g]}{\sum_{j=1}^L w_j^{g-1} K[(\alpha, p_f)_k^g | (\alpha, p_f)_j^{g-1}]} & if\ g = 2, 3, \ldots, G \end{cases}. \tag{35}$$

where π denotes the prior distributions of ρ and p_f. After computing the weights, they are normalized, $w_l^g = w^{*g}_l / (\sum_{l=1}^L w^{*g}_n)$, so that $\sum_{l=1}^L w_l^g = 1$. The total number of generations G is determined by the acceptance rate of each generation, with the algorithm terminating once the acceptance rate drop below 0.5%, which serves as the stopping rule [38]. The pseudo-code for the algorithm is provided below.

Algorithm 1: Pseudo-code of ABC-SMC Algorithm

Input: Data $\{x_1, \cdots, x_n\}$

Output: $L = 5000$ posterior distribution samples $\{(\rho, p_f)_l\}_{l=1}^{L}$

Set the tolerance of the first generation $\epsilon_1 = [\sum_{i=1}^{11}(P_{e,i})^2]^{1/2}$

for *g=1,2,...,G* **do**

  for *l=1,2,...,L* **do**

    while $d_l^g > \epsilon_g$ **do**

      if *g=1* **then**

        Sample ρ^{**} and p_f^{**} independently from prior uniform distributions $U[0,1] \times U[1,8]$ and $U[0,1]$;

      else

        Sample $(\rho, p_f)^*$ from the last generation $\{(\rho, p_f)_l^{g-1}\}_{l=1}^{L}$ with weights $\{w_l^{g-1}\}_{l=1}^{L}$;

        Perturb the sample $(\rho, p_f)^{**} \sim K[(\rho, p_f)^{**}|(\rho, p_f)^*]$;

      end

      Using the model to generate simulated data $\{P'_{e,1}, \ldots, P'_{e,11}\}$ from $f(P_e|(\rho, p_f)^*)$;

      Calculate the distance between the simulated data $\{P'_{e,1}, \ldots, P'_{e,11}\}$ and the observed data $\{P_{e,1}, \ldots, P_{e,11}\}$, $d_l^g = [\sum_{i=1}^{11}(P'_{e,i} - P_{e,i})^2]^{1/2}$;

    end

    Set $(\rho, p_f)_l^g = (\rho, p_f)_l^{**}$ and calculate the weight for each of the accepted samples

    $w_l^g = \begin{cases} 1 & if\ g = 1 \\ \frac{\pi[(\rho,p_f)_l^g]}{\Sigma_{j=1}^{L} w_j^{g-1} K[(\rho,p_f)_l^g|(\rho,p_f)_j^{g-1}]} & otherwise \end{cases}$, where π is the prior distributions;

  end

  Normalize the weights $\{w_l^g\}_{l=1}^{L}$;

  Set the tolerance for the next generation $\epsilon_{g+1} = Median(\{d_l^g\}_{l=1}^{L})$;

end

S1 Fig.

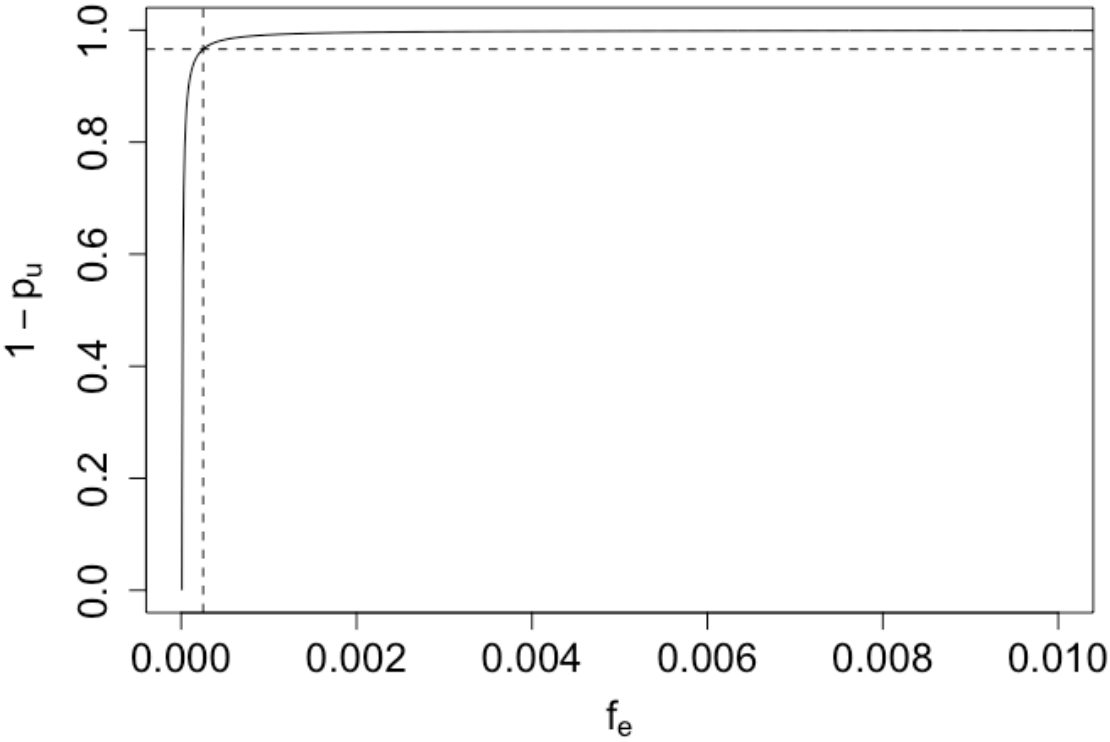

Relationship between f_e and $1 - p_u$. The plot illustrates how changes in f_e influence the variance of the binomial distributions in Eqs. 6–7, which is given by $\mathrm{Var}(G_{\{M,F\}}) = G_{\{M,F\}} f_e p_u (1 - p_u) = G_{\{M,F\}} \frac{V}{V_H}(1 - \frac{V}{V_H f_e}) \propto (1 - p_u)$. The dashed lines represent the benchmark value of f_e and corresponding $1 - p_u$.

S2 Fig.

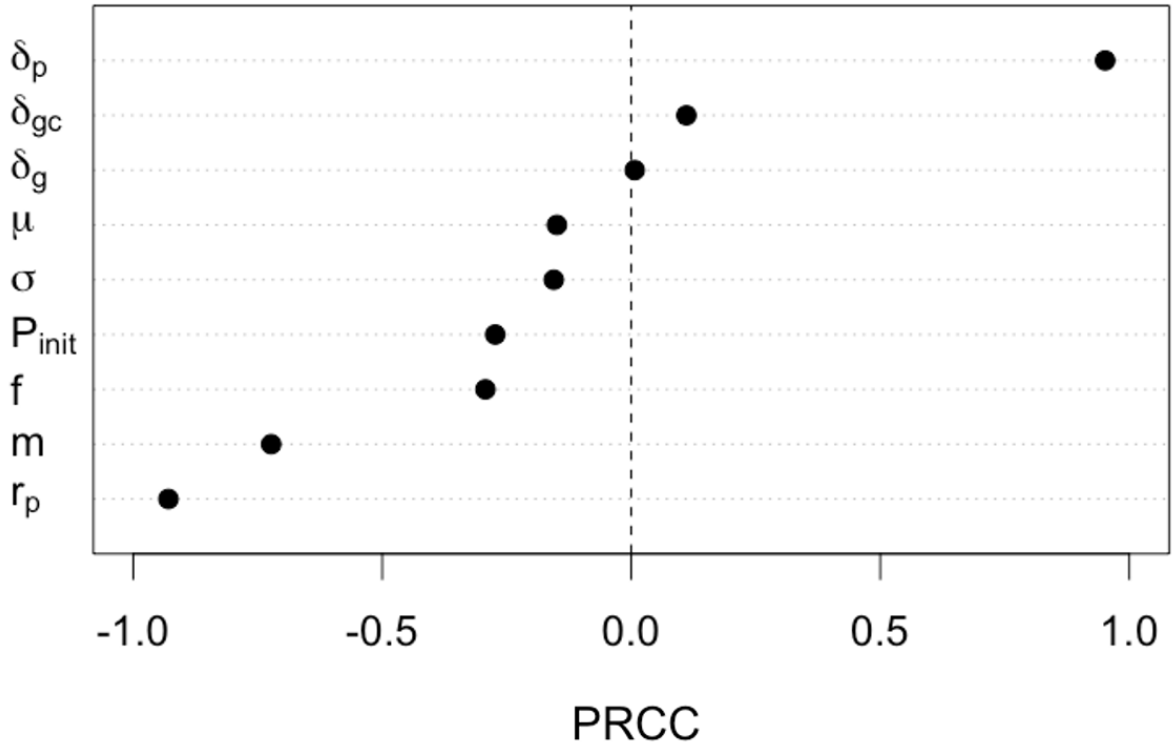

PRCC results between parameters and t_G. The top three parameters that influence the t_G (i.e., those with the largest absolute values) are δ_p (PRCC=0.95), r_p (PRCC=-0.93), and m (PRCC=-0.72).

S3 Fig.

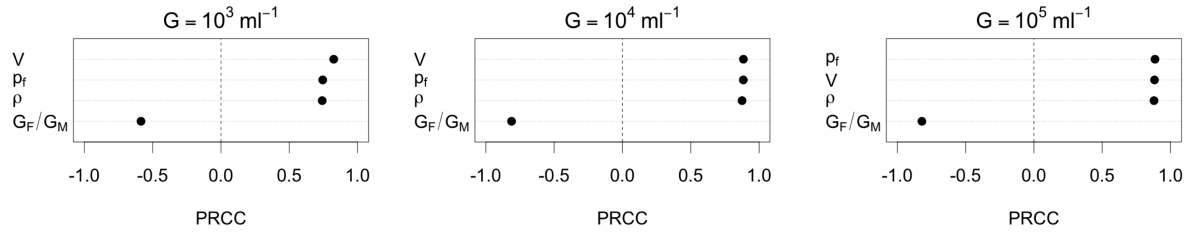

PRCC results between the mosquito parameters and P_i at different gametocytemia level.

S4 Fig.

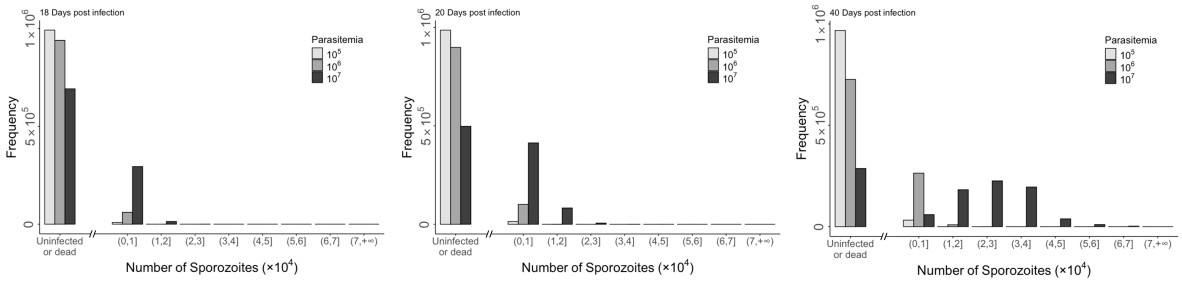

Distributions of salivary gland sporozoites per blood meal in mosquitoes after feeding on humans

with asymptomatic infection at three time points (day 18, 20, 40 post infection).

Acknowledgments

We thank the Australian Research Council (ARC) for supporting this research through Discovery Project DP210101920. We thank Medicines for Malaria Venture for funding the VIS clinical trials. JMM is supported by an ARC Laureate Fellowship (FL240100126). JSM is supported by an NHMRC Investigator Grant (2016396). Computations were conducted on the Nectar Research Cloud, a collaborative Australian research platform supported by the National Collaborative Research Infrastructure Strategy (NCRIS).

References

[1] The World Health Organization. World malaria report 2023. Technical report, World Health Organization, 2023.

[2] G. A. Josling and M Llinás. Sexual development in plasmodium parasites: knowing when it's time to commit. *Nature Reviews Microbiology*, 13(9):573–587, 2015.

[3] Petra Schneider, Louis Clément Gouagna, Sabah Ahmed Omar, Silas Otieno, J. Teun Bousema, Robert W. Sauerwein, and Marga van de Vegte-Bolmer. Submicroscopic plasmodium falciparum gametocyte densities frequently result in mosquito infection. *The American journal of tropical medicine and hygiene*, 76 3:470–4, 2007.

[4] André Lin Ouédraogo, Teun Bousema, Petra Schneider, Sake J. de Vlas, Edith Ilboudo-Sanogo, Nadine Cuzin-Ouattara, Issa Nebie', Will F. G. Roeffen, Jan Peter Verhave, Adrian J F Luty, and Robert W. Sauerwein. Substantial contribution of submicroscopical plasmodium falciparum gametocyte carriage to the infectious reservoir in an area of seasonal transmission. *PLoS ONE*, 4, 2009.

[5] Bronner P. Gonçalves, Melissa C. Kapulu, Patrick Sawa, Wamdaogo Moussa Guelbéogo, Alfred B. Tiono, Lynn Grignard, Will Stone, Joel Hellewell, Kjerstin Lanke, Guido J. H. Bastiaens, John Bradley, Issa Nebie', Joyce Mwongeli Ngoi, Robin M Oriango, Dora Mkabili, Maureen Nyaurah, Janet Midega, Dyann F. Wirth, Kevin Marsh, Thomas S. Churcher, Philip Bejon, Sodiomon B. Sirima, Christopher J. Drakeley, and Teun Bousema. Examining the human infectious reservoir for

plasmodium falciparum malaria in areas of differing transmission intensity. *Nature Communications*, 8, 2017.

[6] Thomas S. Churcher, Teun Bousema, Martin Walker, Christopher J. Drakeley, Petra Schneider, André Lin Ouédraogo, and María-Gloria Basáñez. Predicting mosquito infection from plasmodium falciparum gametocyte density and estimating the reservoir of infection. *eLife*, 2, 2013.

[7] Dari F. Da, Thomas S. Churcher, Rakiswendé Serge Yerbanga, Bienvenue K. Yaméogo, Ibrahim Sangare, Jean-Bosco Ouédraogo, Robert E Sinden, Andrew M. Blagborough, and Anna Cohuet. Experimental study of the relationship between plasmodium gametocyte density and infection success in mosquitoes; implications for the evaluation of malaria transmission-reducing interventions. *Experimental parasitology*, 149:74–83, 2015.

[8] John Bradley, Will Stone, Dari F Da, Isabelle Morlais, Alassane Dicko, Anna Cohuet, Wamdaogo Moussa Guelbéogo, Almahamoudou Mahamar, Sandrine Eveline Nsango, Harouna M Soumare, Halimatou Diawara, Kjerstin H. W. Lanke, Wouter Graumans, Rianne Siebelink-Stoter, Marga G. van de Vegte-Bolmer, Ingrid T Chen, Alfred B. Tiono, Bronner P Gonçalves, Roland D. Gosling, Robert W. Sauerwein, Christopher J. Drakeley, Thomas S. Churcher, and Teun Bousema. Predicting the likelihood and intensity of mosquito infection from sex specific plasmodium falciparum gametocyte density. *eLife*, 7, 2018.

[9] Moshe B Hoshen, Reinhart Heinrich, Wilfred Donald Stein, and Hagai Ginsburg. Mathematical modelling of the within-host dynamics of plasmodium falciparum. *Parasitology*, 121:227 – 235, 2000.

[10] Sompob Saralamba, Wirichada Pan-ngum, Richard James Maude, Sue J Lee, Joel Tarning, Niklas Lindegårdh, Kesinee Chotivanich, François H. Nosten, Nicholas P. J. Day, Duong Socheat, Nicholas J. White, Arjen M. Dondorp, and Lisa Jane White. Intrahost modeling of artemisinin resistance in plasmodium falciparum. *Proceedings of the National Academy of Sciences*, 108:397 – 402, 2010.

[11] Sophie G. Zaloumis, Andrew Jonathan Humberstone, Susan A. Charman, Ric N. Price, Joerg J. Moehrle, Javier Gamo-Benito, James M. McCaw, Kris M. Jamsen, Katherine Smith, and Julie Anne Simpson. Assessing the utility of an anti-malarial pharmacokinetic-pharmacodynamic model for aiding drug clinical development. *Malaria Journal*, 11:303 – 303, 2012.

[12] Martin Eichner, Hans H. Diebner, Louis Molineaux, William E. Collins, Geoffrey M. Jeffery, and Klaus Dietz. Genesis, sequestration and survival of plasmodium falciparum gametocytes: parameter estimates from fitting a model to malariatherapy data. *Transactions of the Royal Society of Tropical Medicine and Hygiene*, 95 5:497–501, 2001.

[13] P. Cao, K. A. Collins, S. Zaloumis, T. Wattanakul, and J. M. Mccaw. Modeling the dynamics of plasmodium falciparum gametocytes in humans during malaria infection. *eLife*, 8, 2019.

[14] Miranda Ijang Teboh-Ewungkem and Thomas Yuster. A within-vector mathematical model of plasmodium falciparum and implications of incomplete fertilization on optimal gametocyte sex ratio. *Journal of theoretical biology*, 264 2:273–86, 2010.

[15] Miranda Ijang Teboh-Ewungkem, Woldegebriel Assefa Woldegerima, and Gideon A. Ngwa. Mathematical assessment of the impact of human-antibodies on sporogony during the within-mosquito dynamics of plasmodium falciparum parasites. *Journal of theoretical biology*, page 110562, 2020.

[16] Lauren M. Childs and Olivia F. Prosper. The impact of within-vector parasite development on the extrinsic incubation period. *Royal Society Open Science*, 7, 2020.

[17] Isaac J. Stopard, Thomas S. Churcher, and Ben Lambert. Estimating the extrinsic incubation period of malaria using a mechanistic model of sporogony. *PLoS Computational Biology*, 2021.

[18] Xiao Sun, James M. McCaw, and Pengxing Cao. Stochastic modeling of within-host dynamics of plasmodium falciparum. *Mathematics*, 10(21), 2022.

[19] Fitsum Girma Tadesse, Lisette Meerstein-Kessel, Bronner P. Gonçalves, Christopher J. Drakeley, Lisa C. Ranford-Cartwright, and Teun Bousema. Gametocyte sex ratio: The key to understanding plasmodium falciparum transmission? *Trends in Parasitology*, 35:226 – 238, 2019.

[20] Luke Anthony Baton and Lisa C. Ranford-Cartwright. Spreading the seeds of million-murdering death: metamorphoses of malaria in the mosquito. *Trends in parasitology*, 21 12:573–80, 2005.

[21] Robert E Sinden. The cell biology of sexual development in plasmodium. *Parasitology*, 86:7 – 28, 1983.

[22] Noriko Okamoto, Timothy P. Spurck, Christopher Dean Goodman, and Geoffrey Ian McFadden. Apicoplast and mitochondrion in gametocytogenesis of plasmodium falciparum. *Eukaryotic Cell*, 8:128 – 132, 2008.

[23] Robert E Sinden, Arthur M. Talman, Sara Rute Marques, Mark N. Wass, and Michael J. E. Sternberg. The flagellum in malarial parasites. *Current opinion in microbiology*, 13 4:491–500, 2010.

[24] Katharine A. Collins, Claire Y. T. Wang, Matthew Adams, Hayley Mitchell, Melanie Rampton, Suzanne Elliott, Isaie J. Reuling, Teun Bousema, Robert W. Sauerwein, Stephan Chalon, Jörg J. Möhrle, and James S. McCarthy. A controlled human malaria infection model enabling evaluation of transmission-blocking interventions. *The Journal of Clinical Investigation*, 128:1551 – 1562, 2018.

[25] Tina Toni, David Welch, Natalja Strelkowa, Andreas Ipsen, and Michael P. H. Stumpf. Approximate bayesian computation scheme for parameter inference and model selection in dynamical systems. *Journal of The Royal Society Interface*, 6:187 – 202, 2008.

[26] Daniel T. Gillespie. Approximate accelerated stochastic simulation of chemically reacting systems. *J. Chem. Phys.*, 115:1716–1733, 2001.

[27] Andargie Abate, Soriya Kedir, Mitiku Bose, Jifar Hassen, Laurent Dembélé, and Lemu Golassa. Infectivity of symptomatic patients and their contribution for infectiousness of mosquitoes following a membrane feeding assay in ethiopia. *Microbiology Spectrum*, 10, 2022.

[28] C. C. Murdock, Eleanore D. Sternberg, and M. Benson Thomas. Malaria transmission potential could be reduced with current and future climate change. *Scientific Reports*, 6, 2016.

[29] Lillian L M Shapiro, Courtney C. Murdock, Gregory R. Jacobs, Rachel J. Thomas, and Matthew B. Thomas. Larval food quantity affects the capacity of adult mosquitoes to transmit human malaria. *Proceedings of the Royal Society B: Biological Sciences*, 283, 2016.

[30] Sandra Bennink, Meike J. Kiesow, and Gabriele Pradel. The development of malaria parasites in the mosquito midgut. *Cellular Microbiology*, 18:905 – 918, 2016.

[31] April M. Clayton, Yuemei Dong, and George Dimopoulos. The anopheles innate immune system in the defense against malaria infection. *Journal of Innate Immunity*, 6:169 – 181, 2013.

[32] Emma Pietsch, Korbinian Niedermüller, Mia Andrews, Britta S. Meyer, Tobias L Lenz, Danny W. Wilson, Tim W. Gilberger, and Paul-Christian Burda. Disruption of a plasmodium falciparum patatin-like phospholipase delays male gametocyte exflagellation. *Molecular Microbiology*, 121:529 – 542, 2023.

[33] Wouter Graumans, Roel Heutink, Geert-Jan van Gemert, Marga G. van de Vegte-Bolmer, Teun Bousema, and Katharine A. Collins. A mosquito feeding assay to examine plasmodium transmission to mosquitoes using small blood volumes in 3d printed nano-feeders. *Parasites & Vectors*, 13, 2020.

[34] Sachie Kanatani, Deborah Stiffler, Teun Bousema, Gayane Yenokyan, and Photini Sinnis. Revisiting the plasmodium sporozoite inoculum and elucidating the efficiency with which malaria parasites progress through the mosquito. *Nature Communications*, 15, 2024.

[35] Scott Anthony Sisson, Y. Fan, and Mark M. Tanaka. Sequential monte carlo without likelihoods. *Proceedings of the National Academy of Sciences*, 104:1760 – 1765, 2007.

[36] Pablo Suárez-Cortés, Giulia Costa, Manuela Andres, Daniel Eyermann, Cornelia Kreschel, Liane Spohr, Christian Goosmann, Volker Brinkmann, and Elena A. Levashina. Generation of a plasmodium falciparum reporter line for studies of parasite biology throughout the life cycle. *bioRxiv*, 2023.

[37] Yannik Schälte and Jan Hasenauer. Informative and adaptive distances and summary statistics in sequential approximate bayesian computation. *PLOS ONE*, 18, 2022.

[38] Maxime Lenormand, Franck Jabot, and Guillaume Deffuant. Adaptive approximate bayesian computation for complex models. *Computational Statistics*, 28:2777–2796, 2013.

[39] Simeone Marino, Ian B. Hogue, Christian J Ray, and Denise E. Kirschner. A methodology for performing global uncertainty and sensitivity analysis in systems biology. *Journal of theoretical biology*, 254 1:178–96, 2008.

[40] Lindsay B Stewart, Aline Fréville, Till S. Voss, David A. Baker, Gordon Akanzuwine Awandare, and David J. Conway. Plasmodium falciparum sexual commitment rate variation among clinical isolates and diverse laboratory-adapted lines. *Microbiology Spectrum*, 10, 2022.

[41] Palang Chotsiri, Almahamoudou Mahamar, Richard M Hoglund, Fanta Koita, Koualy Sanogo, Halimatou Diawara, Alassane Dicko, Julie A. Simpson, Teun Bousema, Nicholas J. White, Joelle M Brown, Roly Gosling, Ingrid T Chen, and Joel Tarning. Mechanistic modeling of primaquine pharmacokinetics, gametocytocidal activity, and mosquito infectivity. *Clinical Pharmacology and Therapeutics*, 111:676 – 685, 2021.

[42] Fitsum Girma Tadesse, Lotus Leonie van den Hoogen, Kjerstin Lanke, Jodie A. Schildkraut, Kevin K.A. Tetteh, Abraham Aseffa, Hassen Mamo, Robert W. Sauerwein, Ingrid Felger, Christopher J. Drakeley, Endalamaw Gadissa, and Teun Bousema. The shape of the iceberg: quantification of submicroscopic plasmodium falciparum and plasmodium vivax parasitaemia and gametocytaemia in five low endemic settings in ethiopia. *Malaria Journal*, 16, 2017.

[43] Hannah C. Slater, Amanda Ross, Ingrid Felger, Natalie E Hofmann, Leanne J. Robinson, Jackie Cook, Bronner P. Gonçalves, Anders Björkman, André Lin Ouédraogo, Ulrika Morris, Mwinyi I. Msellem, Cristian Koepfli, Ivo Mueller, Fitsum Girma Tadesse, Endalamaw Gadisa, Smita Das, Gonzalo J Domingo, Melissa C. Kapulu, Janet Midega, Seth Owusu-Agyei, Cécile Nabet, Renaud Piarroux, Ogobara K. Doumbo, Safiatou Niaré Doumbo, Kwadwo Ansah Koram, Naomi W Lucchi, Venkatachalam Udhayakumar, Jacklin F. Mosha, Alfred B. Tiono, Daniel Chandramohan, Roly Gosling, Felista Mwingira, Robert W. Sauerwein, Richard Paul, Eleanor M. Riley, Nicholas J. White, François H. Nosten, Mallika Imwong, Teun Bousema, Christopher J. Drakeley, and Lucy C. Okell. The temporal dynamics and infectiousness of subpatent plasmodium falciparum infections in relation to parasite density. *Nature Communications*, 10, 2019.

[44] Christina Salgado, George Ayodo, Michael D. Macklin, Meetha P. Gould, Srinivas Nallandhighal, Eliud O. Odhiambo, Andrew Ambogo Obala, Wendy Prudhomme O'Meara, Chandy C. John, and Tuan M. Tran. The prevalence and density of asymptomatic plasmodium falciparum infections among children and adults in three communities of western kenya. *Malaria Journal*, 20, 2021.

[45] Teun Bousema, Lucy C. Okell, Ingrid Felger, and Christopher J. Drakeley. Asymptomatic malaria infections: detectability, transmissibility and public health relevance. *Nature Reviews Microbiology*, 12:833–840, 2014.

[46] Lei Zhu, Jaishree Tripathi, Frances Rocamora, Olivo Miotto, Rob W. van der Pluijm, Till S. Voss, Sachel Mok, Dominic P. Kwiatkowski, François H. Nosten, Nicholas P. J. Day, Nicholas J. White, Arjen M. Dondorp, Zbynek Bozdech, Aung Pyae Elizabeth A. Frank Khin Kyaw Myo M Abul Mayfo Phyo Ashley Smithuis Lin Tun Faiz Mayxay Dhorda Th, Aung Pyae Phyo, Elizabeth A. Ashley, Frank M. Smithuis, Khin Lin, Kyaw Myo Tun, M. Abul Faiz, Mayfong Mayxay, Mehul Dhorda, Nguyen T Thuy-Nhien, Paul N. Newton, Sasithon Pukrittayakamee, Tin Maung Hlaing, Tran Tinh Hien, and Ye Htut. The origins of malaria artemisinin resistance defined by a genetic and transcriptomic background. *Nature Communications*, 9, 2018.

[47] Harvie P. Portugaliza, Shinya Miyazaki, Fiona J. A. Geurten, Christopher Pell, Anna Rosanas-Urgell, Chris J. Janse, and Alfred Cortés. Artemisinin exposure at the ring or trophozoite stage impacts plasmodium falciparum sexual conversion differently. *eLife*, 9, 2020.

[48] Harvie P. Portugaliza, Hamatandi Magloire Natama, Pieter Guetens, Eduard Rovira-Vallbona, Athanase Mwinessobaonfou Somé, Aida Millogo, Delwendé Florence Ouedraogo, Innocent Valéa, Hermann Sorgho, Halidou Tinto, Nguyen Van Hong, António Sitoe, Rosauro Varo, Quique Bassat, Alfred Cortés, and Anna Rosanas-Urgell. Plasmodium falciparum sexual conversion rates can be affected by artemisinin-based treatment in naturally infected malaria patients. *eBioMedicine*, 83, 2022.

[49] Will Stone, Joseph J. Campo, André Lin Ouédraogo, Lisette Meerstein-Kessel, Isabelle Morlais, Dari F. Da, Anna Cohuet, Sandrine Eveline Nsango, Colin J. Sutherland, Marga van de Vegte-Bolmer, Rianne Siebelink-Stoter, Geert-Jan van Gemert, Wouter Graumans, Kjerstin Lanke, Adam D. Shandling, Jozelyn V. Pablo, Andy Teng, Sophie Jones, Roos M. de Jong, Amanda Fabra-García, John Bradley, Will F. G. Roeffen, Edwin Lasonder, Giuliana Gremo, Evelin Schwarzer, Chris J. Janse, Susheel Kumar Singh, Michael Theisen, Philip L. Felgner, Matthias Marti, Christopher J. Drakeley, Robert W. Sauerwein, Teun Bousema, and Matthijs M. Jore. Unravelling the immune signature of plasmodium falciparum transmission-reducing immunity. *Nature Communications*, 9, 2018.

[50] André Lin Ouédraogo, Will F. G. Roeffen, Adrian J F Luty, Sake J. de Vlas, Issa Nebie', Edith Ilboudo-Sanogo, Nadine Cuzin-Ouattara, Karina Teleen, Alfred B. Tiono, Sodiomon Bienvenu Sirima, Jan Peter Verhave, Teun Bousema, and Robert W. Sauerwein. Naturally acquired immune responses to plasmodium falciparum sexual stage antigens pfs48/45 and pfs230 in an area of seasonal transmission. *Infection and Immunity*, 79:4957 – 4964, 2011.

[51] Nicholas J. White. Primaquine to prevent transmission of falciparum malaria. *The Lancet. Infectious diseases*, 13 2:175–81, 2013.

[52] Mayumi Tachibana, Eizo Takashima, Motomi Torii, Yimin Wu, Jetsumon Sattabongkot, and Takafumi Tsuboi. Advances in transmission-blocking vaccines against plasmodium falciparum and plasmodium vivax. *Expert review of vaccines*, 2025.

[53] Martin K. Rono, Mary Akinyi Nyonda, Joan Simam, Joyce Mwongeli Ngoi, Sachel Mok, Moses Mosobo Kortok, Abdullah S. Abdullah, Mohammed Elamin Mustafa Elfaki, John N. Wait-

umbi, Ibrahim M. El-Hassan, Kevin Marsh, Zbynek Bozdech, and Margaret J. Mackinnon. Adaptation of plasmodium falciparum to its transmission environment. *Nature Ecology & Evolution*, 2:377 – 387, 2017.

[54] Aissata Barry, John Bradley, Will Stone, Moussa W. Guelbeogo, Kjerstin Lanke, Alphonse Ouédraogo, Issiaka Soulama, Issa Nebie', Samuel Sindié Sermé, Lynn Grignard, Catriona Patterson, Lindsey Wu, Jessica Briggs, Owen Janson, Shehu Shagari Awandu, Mireille Ouédraogo, Casimir Tarama, Désiré Kargougou, Soumanaba Zongo, Sodiomon Bienvenu Sirima, Matthias Marti, Christopher J. Drakeley, Alfred B. Tiono, and Teun Bousema. Higher gametocyte production and mosquito infectivity in chronic compared to incident plasmodium falciparum infections. *Nature Communications*, 12, 2021.

[55] Chiara Andolina, Jordache Ramjith, John Rek, Kjerstin Lanke, Joseph Okoth, Lynn Grignard, Emmanuel Arinaitwe, Jessica Briggs, Jeffrey A. Bailey, Ozkan Aydemir, Moses R. Kamya, Bryan Greenhouse, Grant Dorsey, Sarah G. Staedke, Christopher J. Drakeley, Marianne Jonker, and Teun Bousema. Plasmodium falciparum gametocyte carriage in longitudinally monitored incident infections is associated with duration of infection and human host factors. *Scientific Reports*, 13, 2023.

[56] Arthur Lensen, M Bolmer-Van de Vegte, Geert-Jan van Gemert, Wijnand M. C. Eling, and Robert W. Sauerwein. Leukocytes in a plasmodium falciparum-infected blood meal reduce transmission of malaria to anopheles mosquitoes. *Infection and Immunity*, 65:3834 – 3837, 1997.

[57] Louis Clément Gouagna, Heather M. Ferguson, Bernard A. Okech, Gerard F. Killeen, Ephantus Wanjohi Kabiru, John C. Beier, John I. Githure, and Guiyun Yan. Plasmodium falciparum malaria disease manifestations in humans and transmission to anopheles gambiae: a field study in western kenya. *Parasitology*, 128:235 – 243, 2004.

[58] Yuemei Dong, Ruth Aguilar, Zhiyong Xi, Emma Warr, Emmanuel Mongin, and George Dimopoulos. Anopheles gambiae immune responses to human and rodent plasmodium parasite species. *PLoS Pathogens*, 2, 2006.

[59] Emma J Dawes, Thomas S. Churcher, Shijie Zhuang, Robert E Sinden, and María-Gloria Basáñez. Anopheles mortality is both age- and plasmodium-density dependent: implications for malaria transmission. *Malaria Journal*, 8:228 – 228, 2009.

[60] Sarah Filippi, Chris P. Barnes, Julien Cornebise, and Michael P.H. Stumpf. On optimality of kernels for approximate bayesian computation using sequential monte carlo. *Statistical Applications in Genetics and Molecular Biology*, 12(1):87–107, 2013.